Midbrain dopamine drives splenic immunity through a brain-to-body circuit

Adithya Gopinath[1,2]*, Alfonso Apicella[3], Aidan Smith[1], Alice Bertero[3], Elijah Freedman[1], Lauryn Hornstein[1], Logan Wood[1], Hannah Ciupe[1], Delaney Booth[1], Sabrina Campos[1], Nirvana Soundara[1], Daniel L. Purich[4], Pedro Trevizan-Baú[5], Leah R. Reznikov[5], Nikhil Urs[6], Olga Guryanova[6], Daniel W. Wesson[6], Habibeh Khoshbouei[1]*

*Co-Corresponding Authors

1- Department of Neuroscience, University of Florida, Gainesville FL USA
2- Department of Neurology, University of Florida, Gainesville, FL USA
3- University of Texas San Antonio, San Antonio, Texas USA
4- Department of Biochemistry and Molecular Biology, University of Florida, Gainesville FL USA
5- Department of Physiological Sciences, University of Florida, Gainesville FL USA
6- Department of Pharmacology and Therapeutics, University of Florida, Gainesville FL USA

Funding: This work was supported by NIH grants to Habibeh Khoshbouei (H.K.): R01NS071122-07A1 (to H. K.), R01DA026947-10, National Institutes of Health Office of the Director Grant 1S10OD020026-01 (to H. K) R01DA058143-02 (to H.K.), R21NS133384-01 (to H.K.), Evelyn F. and William L. McKnight Brain Institute's Gator Neuroscholars Program (to A.G.), and the Karen Toffler Charitable Trust (to A.G.).

Abstract
Midbrain dopamine neurons are well-known to shape central nervous system function, yet there is growing evidence for their influence on the peripheral immune systems. Here we demonstrate that midbrain dopamine neurons form a circuit to the spleen via a multisynaptic pathway from the dorsal vagal complex (DVC) through the celiac ganglion. Midbrain dopamine neurons modulate the activity of D1-like and D2-like dopamine receptor-expressing DVC neurons. *In vivo* activation of midbrain dopamine neurons induced dopamine release in the DVC and increased immediate early gene expression in both the DVC and celiac ganglion, indicating enhanced neuronal activity. Activation of this midbrain-to-spleen circuit reduced spleen weight and decreased naïve $CD4^+$ T-cell populations without affecting total T-cell numbers. These findings unveil a functional midbrain-DVC-celiac ganglion-spleen pathway, through which midbrain dopamine neurons modulate splenic immunity. These novel insights into the neural regulation of the immune system have important implications for diseases involving altered dopamine neurotransmission and highlight potential targets for immunotherapeutic interventions.

Introduction
While midbrain dopamine neurons play pivotal roles in central and peripheral regulation, the precise circuits connecting them to peripheral immune organs remain largely undefined. While substantial progress has been made in unraveling body-to-brain communication[1], the reverse pathway – how the brain influences peripheral organs, particularly through dopamine signaling – remains unclear. Emerging evidence highlights the brain's significant influence on peripheral systems, particularly in the context of neuroimmune interactions. Zhu and colleagues[2], for instance, identified a functional link between CNS pain processing and splenic immunity, suggesting that neural pathways involved in immune regulation extend well beyond the brain's immediate environment to influence key organs, such as the spleen. Such findings imply that midbrain dopaminergic neurons may play a previously uncharacterized role in orchestrating peripheral immune responses. In Parkinson's disease (PD), degeneration of midbrain dopamine neurons is closely associated with changes in peripheral immune dysfunction believed to

contribute to disease progression[3-5]. Similarly, psychostimulant-induced activation of midbrain dopamine neurons has been shown to regulate peripheral immunity and influence wound healing[6-9]. Moreover, the well-characterized connection between peripheral inflammation and infection, -manifesting in symptoms such as anhedonia and reduced motivation[10-12], strongly suggest a link between dopamine neurotransmission and peripheral immunity. Despite such findings, the specific circuits through which midbrain dopamine neurons communicate with peripheral immune organs remain undefined.

The vagus nerve is one of the most well-characterized brain-body communication routes, connecting the brainstem to multiple peripheral organs, including heart, lung, gut, and spleen[13-15]. The dorsal vagal complex (DVC) plays a pivotal role in modulating immune function through the cholinergic anti-inflammatory pathway[16-18]; however, while body-to-brain communication through vagal afferents has been extensively studied, brain-to-body circuits are less understood. While vagal afferent pathways convey information from the periphery to the brain, the corresponding brain-to-periphery circuits that mediate the brain's control over immune functions through dopamine signaling remain unclear.

Recent advances in neuroanatomical tracing techniques, including optogenetics, have begun to shed light on brain-to-body circuits. Our findings suggest that midbrain dopamine neurons project to the DVC, a brainstem region that acts as a critical relay station for communication between the brain and peripheral organs. The DVC includes the dorsal motor nucleus of the vagus (DMV), and nucleus of the solitary tract (NTS) and is optimally positioned to transmit signals from midbrain dopamine neurons to peripheral organs.

In this study we investigated these pathways by mapping the connections from midbrain dopamine neurons to peripheral immune organs by focusing on how dopamine signaling modulates immune function. The prime objective was to identify these neural circuits in the context of their functional roles in immune regulation. Secondarily, we aimed to shed new insight into diseases like PD and other conditions involving both neurological and immune dysfunction that is linked to dysregulation of CNS dopamine transmission. We successfully mapped the circuitry connecting midbrain dopamine neurons to peripheral immune organs, with particular focus on the spleen, a key organ in immune regulation. Using Cre-dependent viral tracers and chemogenetic approaches, we demonstrated that midbrain dopamine neurons project to the DVC, subsequently relaying through the celiac ganglia to reach the spleen. Furthermore, we investigated how the activation of this circuit influences peripheral immune function, particularly examining the role of midbrain dopamine neuron activity in regulating spleen weight and splenic T-cell populations. The spleen is innervated by both cholinergic[19-21] and catecholaminergic[22-25] fibers, which play critical roles in modulating splenic function, immune cell populations, and the broader peripheral immune landscape. While our findings indicate that midbrain dopamine neuronal activity influences splenic immunity, this effect is unlikely to result from direct dopaminergic innervation of the spleen. Instead, it is more plausible that midbrain dopaminergic projections regulate DVC activity. Adrenergic and cholinergic fibers downstream of the DVC, acting via the celiac ganglion to innervate the spleen, likely mediate the observed immunophenotypic changes associated with midbrain dopamine neuron activation.

Collectively our findings provide novel insights into the neural mechanism underlying the regulation of peripheral immunity by midbrain dopamine neurons, shedding light on the interplay between central dopamine signaling and peripheral immunity. These discoveries hold significant implications for understanding conditions such as Parkinson's Disease, psychostimulant addiction, and immune-mediated disorders- pathologies where dysregulated CNS dopamine signaling may contribute to altered peripheral immune responses.

Results and Discussion

Anterograde mapping of midbrain dopaminergic neurons reveals projections to the dorsal vagal complex.

Accumulating evidence suggests that the brain communicates with the peripheral immune system and influences immune responses. The vagus nerve is a fundamental biological pathway for relaying information between the brain and the periphery. As the primary integrative hub of the mammalian autonomic nervous system, the Dorsal Vagal Complex (DVC) comprises the area postrema (AP), nucleus of the solitary tract (NTS), and dorsal motor nucleus of the vagus (DMV). This anatomical and functional arrangement positions the DVC as a likely relay point for signals from midbrain dopamine neurons to the periphery[1,2,26-28].

To probe whether midbrain dopamine neurons project to the DVC, we utilized DAT-cre mice, which express Cre-recombinase under the control of the dopamine transporter (DAT) promoter[29]. We targeted dopamine neurons by stereotactic injection of AAV2-DIO-eYFP into the midbrain at coordinates -3.4AP, ±0.4ML, -4.4DV (mm from Bregma), resulting in Cre-dependent, monosynaptic anterograde expression of enhanced Yellow Fluorescent Protein (eYFP) (Figure 1A). After allowing three weeks for viral expression, we assessed whether DAT+ midbrain dopamine neurons form projections to the DVC, and the co-expression of eYFP and tyrosine hydroxylase (TH) in the midbrain injection site and in the median forebrain bundle, the latter a well-characterized projection region for midbrain dopamine neurons. Our data confirm the specificity of viral expression within dopamine neurons (Figure 1B, C, and D, Supplementary Figure 1). Notably, we also observed eYFP+ expression throughout the DVC, including in the DMV and NTS, indicating that midbrain DAT+ neurons send synaptic projections to the DVC.

After identifying monosynaptic projections from midbrain dopamine neurons to the DVC (Figure 1), we investigated whether these projections form synapses within the DVC. Using a complementary viral tracing approach (Figure 2A), DAT-cre mice were injected with a Cre-dependent AAV expressing mRuby-tagged Synaptophysin in the midbrain. This fusion protein fluorescently labels synapses originating from midbrain dopamine neurons[30]. mRuby-tagged synaptophysin expression was confirmed at the injection site in the midbrain as well as and in known projection areas, such as the striatum (Figure 2B, 2C, Supplemental Figure 2). As the most specific indicator for identifying cholinergic neurons, choline acetyltransferase (ChAT) co-staining was used to identify the DVC (Figure 2D). mRuby+ puncta were observed throughout the DVC, including in the DMV and NTS (Figure 2E), indicating that DAT+ midbrain dopamine neurons not only project to the DVC, but also form synapses within the DVC and its subnuclei. These findings support a two-part hypothesis: 1) changes in midbrain dopamine neuron activity and dopamine release at these synapses modulate DVC neuronal activity; and 2) this modulation, in turn, regulates peripheral systems downstream of the DVC in a previously unrecognized component of the midbrain dopamine neuron-to-peripheral immunity circuit.

DVC neurons express D1-like and D2-like receptors.

For the DVC neurons to respond to dopaminergic input, it is critical to demonstrate functional D1-like or D2-like dopamine receptor in the DVC in the DVC. Therefore, we performed whole-cell patch-clamp recordings on GFP-expressing ChAT+ neurons in the 250um coronal sections containing the DVC from ChAT-GFP mice. This approach enabled us to measure the effect of dopamine on the biophysical properties of these neurons, offering mechanistic insights into dopaminergic modulation within the DVC. Recordings were conducted on 250um coronal brain slices containing the DVC, with synaptic inhibitors applied to block GABAergic and glutamatergic signaling (Figure 3A). Although, at a population level, dopamine had no significant effect on DVC ChAT-GFP neurons in passive (Figure 3B) or active (Figure 3C) properties, two populations with opposing responses were identified. The first (Figure 3D) reacted with a significant lowering of rheobase and an increased F/I slope, while no changes in synaptic integration were observable. Such behavior indicates an enhanced excitability following dopamine administration, consistent with the expression of D1 receptors. Bath application of D1

receptor antagonists (SCH23390 10μM) restored the baseline conditions (data not shown). High concentration dopamine perfusion (50 μM) resulted in higher rheobase, a reduced F/I slope, and a critically impaired synaptic integration with reduced summation upon consecutive EPSP-like stimuli, which further reduced the neuron excitability, in the second population. These responses were compatible with D2 receptor expression. Bath application of Eticlopride (10μM), a selective D2 receptor antagonist, restored baseline conditions. Overall, these results suggest that dopamine modulates at least two subpopulations of ChAT+ neurons in the DVC. Particularly, these findings indicate that ChAT+ neurons in the DVC, which receive projections and synapses from midbrain dopamine neurons, are responsive to dopamine, enhancing the excitability of D1-expressing neurons and reducing the excitability of D2-expressing neurons. These findings support the hypothesis that the DVC acts as a relay structure, linking midbrain dopamine neuronal activity to the DVC and peripheral systems downstream of the DVC.

Chemogenetic stimulation of midbrain dopamine neuron induces dopamine release in the DVC.

Our findings show that midbrain dopamine neurons project to the DVC and that exogenous dopamine application evokes canonical D1R- or D2R-mediated responses in DVC neurons expressing these receptors. Building on these data, we tested the hypothesis that stimulation of midbrain dopamine neurons causes dopamine release in the DVC, a downstream projection site. To address this hypothesis, the midbrain of DAT:cre mice (Figure 4A) received intracranial injection of Cre-dependent mCherry-tagged AAV-DIO-Gq-DREADD that signal through the Gαq/11 G-protein leading to neuronal activation via stimulating phospholipase C and increased intracellular calcium[31-33]. Three weeks post-injection, the AAV DIO-mediated expressions of Gq-DREADD-mCherry were verified in the somatic (midbrain) and terminal regions (striatum and DVC) (Figure 4, Supplementary Figure 3). Gq-DREADD-mCherry expression in the midbrain and striatal projection served as positive controls (Supplementary Figure 3).

In a separate cohort, we injected AAV-Dio-Gq-DREADD-mCherry into the midbrain and AAV9-hSyn-dLight1.3b in the DVC, leading to the expression of the high-affinity dopamine sensor dLight1.3b[34] in the DVC (Figure 4A). Three weeks later, 250-μm coronal slices of the DVC were imaged via one-photon slice-imaging. After a 30-second baseline, bath perfusion with 10 μM clozapine-*N*-oxide (CNO), a synthetic agonist of human muscarinic receptors, significantly increased dLight1.3b fluorescence (Figure 4D). These data indicate that dopamine is released from Gq-DREADD-expressing midbrain originated dopamine terminals in the DVC.

To validate the dopamine-specific dLight1.3b signal, DVC sections were imaged at baseline and after perfusion with either 10 μM methamphetamine, a well-characterized stimulator of dopamine release[35-37], or 0.1 μM dopamine. Both treatments significantly increased dLight1.3b fluorescence (Figure 4E, 4F), confirming the specificity of dopamine release from dopaminergic terminals in the DVC. These findings support the conclusion that chemogenetic stimulation of midbrain dopamine neurons induces dopamine release in the DVC. This finding suggests that dopaminergic projections from the midbrain regulate DVC activity - and through downstream adrenergic and cholinergic fibers - via the vagus nerve and celiac ganglion, ultimately modulate peripheral immunity.

Anterograde multi-transsynaptic tracing reveals midbrain-to-spleen connectivity via celiac ganglion.

Top-down regulation of peripheral functions by the CNS is a fundamental principle in neuroscience and determining the circuits connecting specific brain regions to peripheral immune functions is essential for understanding neurological and neuropsychiatric disorders. Recent studies show that CNS connections to the spleen mediate pain-induced peripheral immune responses[2]. The celiac ganglion, which receives projections from the DVC, acts as a relay to peripheral organs, including the liver, bone marrow, and spleen[38-42]. Vagal afferents via the celiac

ganglion regulate splenic immune functions[23,43-46]. Our findings, along with those of others[47,48], demonstrate that midbrain dopamine neuron activity modulates peripheral immunity, although the precise circuitry remains unclear. Decades of research support the existence of the celiac ganglia-DVC circuit[49,50], and with the midbrain dopamine neuron-to-DVC projections identified in this study, we propose a multi-synaptic link between midbrain dopamine neurons and the spleen.

To investigate this sub-hypothesis, we used Ai9 mice, where fluorescent TdTomato, itself a tandem dimer of two RFP subunits, is expressed in neurons transduced to express Cre recombinase. We performed midbrain injections of anterograde AAV1-Cre to induce Cre expression that transduce in a multi-transsynaptic manner (Figure 5A). Three weeks later, TdTomato+ cells were observed in the DVC, celiac ganglion, and spleen (Figure 5C-E). Although these results indicate a midbrain-DVC-celiac ganglion-spleen pathway, they do not exclude the possibility that other connections may also influence peripheral immunity[51,52]. The midbrain-DVC-celiac ganglion-spleen pathway offers a potential mechanism by which midbrain dopamine neuron activity may influence splenic immune function. To explore this possibility, we developed a stepwise experimental approach to investigate the functional impact of midbrain dopamine neuron activation at each junction of this circuit.

Chemogenetic stimulation of midbrain dopamine neurons modulates downstream projection regions, as measured by increased cFos expression in the DVC.

Thus far we have shown that: 1) midbrain dopamine neurons project to and release dopamine in the DVC; 2) DVC neurons are capable of responding to dopaminergic input, and 3) multi-synaptic projections exist from the midbrain to the spleen via a midbrain-DVC-celiac ganglion-spleen circuit. It stands to reason that activation of midbrain dopamine neurons, and subsequent dopamine release in the DVC, would increase neuronal activity along the midbrain-DVC-celiac ganglion axis, potentially resulting in splenic immunological changes. Immunostaining for cFos expression, an immediate-early gene induced by neuronal activity that reaches peak expression within 90 minutes after neuronal activation[53-56] is a reliable approach to measure increased neuronal activity along the midbrain-DVC-celiac ganglion axis. We tested the hypothesis that dopamine neuron activation would result in increased DVC and celiac ganglion neuronal activity.

We injected AAV:Dio:Gq DREADDs-mCherry or AAV-Dio-mCherry (control) into the midbrain of DAT:cre mice. Three weeks post-injection, the mice received daily intraperitoneal injections of clozapine-N-oxide (CNO; 1 mg/kg) for 14 days to activate the DREADDs (Figure 6A). Locomotor activity, a reliable readout of dopamine neuron activation, was assessed at baseline and following CNO injections on Days 1, 7, and 13 (Supplementary Figure 5; Supplemental Video 1). Consistent with our hypothesis, mice injected with AAV:Dio:Gq DREADDs-mCherry exhibited significantly increased locomotor activity in response to CNO, confirming activation of midbrain dopamine neurons (Supplementary Figure 5B-C). Additionally, we observed a robust increase in cFos expression in the dorsal vagal complex (DVC), particularly within the dorsal motor nucleus of the vagus (DMV) and nucleus tractus solitarius (NTS) subregions (Figure 6). This effect was absent in the empty-vector control group (Figure 6B-D). These findings demonstrate that activation of midbrain dopamine neurons influences neuronal activity along the midbrain-DVC axis, as evidenced by the observed increases in cFos expression.

To further investigate downstream effects of midbrain dopamine neuron activation, we assessed cFos expression in the celiac ganglia of mice injected with excitatory DREADDs, compared to the empty vector control following systemic CNO administration (Figure 7A). Intact celiac ganglia were dissected, whole-mounted, post-fixed, and immunostained, followed by confocal microscopy. Consistent with the proposed midbrain-DVC-celiac ganglion circuitry, we observed increased neuronal activity, as evidenced by elevated cFos expression in Gq DREADD-injected mice, compared to the empty vector control (Figure 7B-C). Quantification revealed a marked increase in cFos+ cells in Gq-DREADD-treated mice relative to controls (Figure 7D). These results support the interpretation that midbrain dopamine neuron activity functionally

regulates splenic immunity via a midbrain-DVC-celiac ganglion-spleen circuitry. Together, these findings demonstrate that midbrain dopamine neuron activation profoundly influences neuronal activity along the midbrain-DVC axis and downstream autonomic circuits, highlighting a functional role in regulating peripheral immune responses.

Chemogenetic stimulation of midbrain dopamine neurons reduces spleen weight and naïve CD4+ T-cell populations without affecting total cell numbers

As a key immune organ, the spleen plays a central role in orchestrating both innate and adaptive immune responses, responding to pathogens, immune activation, and even cancer[57-64]. Disruptions in splenic immune cell populations or function, due to altered CNS dopamine neurotransmission, could have profound immunological consequences. Such behavior is particularly relevant in diseases characterized by dysregulated dopamine neuron activity and existing peripheral immune disturbances, potentially influenced by CNS dopamine signaling. For instance, PD, conventionally defined by the loss of midbrain dopamine neurons and motor deficits, also exhibits peripheral immune manifestations, including changes in the phenotype of immune cell populations, gut dysfunction, and systemic inflammation[3-5,65], with PD patients exhibiting impaired CD4+ T-cell migration, accompanied an increase total CD4+ T-cell populations[65-67]. Conversely, psychostimulant use, which elevates brain dopamine levels, leads to opposing T-cell responses, including a reduction in total T-cells, and an increased propensity towards inflammatory T-cell phenotypes[68-72].These observations suggest that changes in CNS dopamine transmission – whether through loss, as in PD, or through augmentation, as seen with psychostimulants – can significantly influence immune function[65-67, 68-72]. The interplay between midbrain dopamine neuron activity and peripheral immune responses underscores a relationship where CNS signaling impacts systemic immunity[6,47,48,73,74]. To probe whether the midbrain-DVC-celiac ganglion-spleen circuit modulates splenic immunity, we assessed splenic immune cell populations following the activation of midbrain dopamine neurons. Using DATcre mice expressing Cre-dependent Gq DREADDs or empty vector control, we administered daily CNO (1 mg/kg) injections for 14 days to selectively stimulate DAT+ midbrain dopamine neurons (Figure 7A). Spleens harvested from mice with activated midbrain dopamine neurons displayed significantly reduced weight compared to controls (Figure 7B), reinforcing the idea that midbrain dopamine signaling influence splenic immune function. These data are consistent with previous studies in DAT-knockout (DAT-KO) mice, marked by elevated CNS dopamine, exhibit spleen hypoplasia, reduced spleen weight[74,75]. Following spleen harvest, we dissociated and immunophenotyped the splenic cells, using flow cytometry to analyze various T-cell populations, including CD4+, CD8+, effector-memory, central memory, and naïve T-cells (Figure 7C-H, Supplemental Figure 6). While total CD4+ and CD8+ T-cell numbers did not differ significantly between the Gq DREADD and control groups (Figure 7I & M), there was a significant reduction in naïve CD4+ T-cells (CD4+, CD62L+, CD44-) in mice with midbrain dopamine neuron activation (Figure 7E-F). Interestingly, similar reductions were not observed in CD8+ T-cell subpopulations (Figure 7G-H). While the stress hormone corticosterone, analogous to human cortisol, can also produce immunological effects, we found no significant changes in corticosterone levels in mice that received Gq DREADDs versus empty vector control, suggesting that the observed effects are independent of corticosterone's immunomodulatory role (Supplemental Figure 7). Collectively, these findings suggest a targeted modulation of immune cell populations, rather than global suppression, shedding light on mechanisms by which altered dopamine neurotransmission influences peripheral immune function. Importantly, our results align with previous studies demonstrating that top-down regulation of splenic T-cells can affect peripheral immune manifestations such as pain[48]. Additionally, dopamine neuron activation has been shown to modulate immune populations such as myeloid-derived suppressor cells (MDSCs), which inhibit the differentiation of naïve CD4+ T-cells into regulatory phenotypes[48]. Notably, increasing peripheral MDSCs through dopamine neuron activation has been associated with anti-tumor

effects. [48] These findings underscore the potential therapeutic implications of midbrain dopamine neuron modulation in diseases involving immune dysfunction.

Through celiac ganglia innervation, the spleen is innervated by both cholinergic[19-21] and catecholaminergic[22-25] fibers, both of which can modulate spleen function, immune cell populations, and by extension influence the peripheral immune landscape. Though we found that midbrain dopamine neuronal activity can modulate splenic immunity, this is unlikely to be due to dopaminergic innervation of the spleen[76-78]. Instead, dopaminergic projections from midbrain are more likely to regulate DVC activity, with downstream adrenergic and cholinergic fibers, via the vagus nerve and celiac ganglion, ultimately modulating splenic immunity. This pathway likely underpins the immunophenotypic changes observed following midbrain dopamine neuron activation. The central finding of our study is that activation of midbrain dopamine neurons induces functional immunological changes in the spleen.

The DVC, which contains multiple vagal nuclei upstream of the periphery, projects to numerous peripheral organs via the vagal efferent pathway. This raises the possibility that the changes in splenic immunity observed upon chemogenetic activation of midbrain dopamine neurons may also reflect alterations in the activity of other peripheral organs outside the proposed midbrain-DVC-celiac ganglion-spleen circuit[28,38,79,80].

Future studies will focus on chemogenetic or optogenetic stimulation of the DVC, bypassing the midbrain, to further define the specificity of the midbrain-DVC-celiac ganglion-spleen pathway. Selectively blocking individual nodes within the pathway will also help clarify the mechanisms underlying midbrain regulation of splenic immunity. For example, if inhibition of DVC activity during midbrain dopamine neuron activation reduces or abolishes the observed changes in splenic CD4+ T-cell populations, this would strongly support the role of the DVC as a critical relay in the circuit.

Overall, this study provides evidence for a functional connection between the CNS and peripheral immunity through midbrain dopamine signaling, revealing a pathway that could be leveraged to modulate immune function in both health and disease. Our findings suggest that midbrain dopamine neuron activation not only affects splenic weight and T-cell populations but also underscores a broader role for dopamine signaling in regulating peripheral immunity. These results have significant translational implications for diseases involving altered dopamine neurotransmission, such as Parkinson's disease and neuropsychiatric disorders. Furthermore, they highlight the potential for targeting dopamine-related pathways in the development of novel immunotherapies and neuroimmunological interventions.

Concluding remarks

In neurophysiology, organ homeostasis is achieved by autonomic pathways that control responses to stimuli, whereby sensory neurons provide body-to-CNS status reports, with CNS and motor neurons projecting regulatory signals to target organs/tissues[81-83]. Disruptions in brain-body communication have been implicated in various diseases, including neurodegenerative disorders like PD[3], cardiovascular diseases[84-86], and metabolic syndromes[87,88]. Integration of the respective afferent and efferent signals allows for rapid, reflexive adaptation to changing demands on organs/tissues. Jin, Li, Jeong, *et al.* (2024) recently demonstrated a body–brain circuit, whereby pro-inflammatory and anti-inflammatory cytokines communicate via distinct populations of vagal neurons to inform the brain of an emerging inflammatory response[1]. While numerous studies have shown that altered dopamine neurotransmission is linked to changes in peripheral immunity, such as during psychostimulant use and degeneration of dopamine neurons in Parkinson's disease[6,65,73,74,89-91], prior evidence for the circuitry between midbrain dopamine neurons and the immune system was scant. In the present study, we now demonstrate the existence of a multi-synaptic brain-to-periphery pathway, linking midbrain dopamine neurons to the dorsal vagal complex (DVC) and spleen, via the celiac ganglia.

Midbrain-originating dopamine signaling emerges as a key modulator of peripheral immunity, with the observed reduction in spleen weight and alterations in T-cell populations—particularly the decrease in naïve CD4+ T-cells, following chemogenetic activation of midbrain dopamine neurons. These results emphasize the influence of midbrain dopamine neurons on adaptive immune functions, with broad implications for conditions like Parkinson's disease and neuropsychiatric disorders, where immune dysregulation and chronic inflammation are central to disease manifestation and progression. Furthermore, dopamine-driven modulation of splenic immune cell populations suggests that midbrain dopamine neuron activity may extend its regulatory effects to immune responses throughout the body. A multitude of diseases, from autoimmunity to cancer, are treated using immunomodulatory drugs, modulating the immune response as a treatment method. Given that dopamine neuron activity modulates spleen T-cell populations, we pondered the possibility that peripheral immunomodulation could also modulate CNS dopamine neurotransmission, via the same circuit. It is well known that during infection and inflammation, patients experience a lack of motivation, social withdrawal, and anhedonia[10,92-94]. Therefore, it is reasonable to postulate that peripheral immunomodulation, via drugs that target the immune system, may function in a feedback/feedforward loop to modulate CNS dopamine neurotransmission. Future studies employing clinically relevant immunomodulatory drugs, or experimental methods such as chemogenetic manipulation of the spleen, will help clarify this compelling question.

Finally, there remains the important and broad question: Why has a biological circuit evolved in the mammalian system to link midbrain dopamine neurons to the peripheral immune system. Dopamine neurotransmission is fundamentally involved in socially motivated behaviors, such as bonding between members of a community and/or between parents/offspring[95-99]. Such behaviors are conserved among various species. Indeed, in the absence of rewarding behaviors, such as during depression, peripheral inflammation and immune dysfunction is increased[100,101]. Thus, midbrain dopaminergic neuronal regulation of the peripheral immune system may facilitate immunity through socialization and bonding reward mechanisms. This idea is supported by the literature that shows activation of midbrain dopamine neurons to promote resolution of infection[47], improve anti-tumor immunity[48], and enhance stress resilience in individuals experiencing chronic stress[102,103], emphasizing the function of dopaminergic signaling in peripheral immunity along the midbrain-spleen axis. In summary, our study highlights the critical role of midbrain dopamine neurons beyond CNS neurotransmission, positioning them as an important regulator of peripheral immunity. This strengthens the concept of brain-body communication, linking neuroimmune interactions to the onset and progression of systemic diseases, and offers promising new pathways for therapeutic interventions targeting these circuits.

Limitations of the methodology and systems used in this study

In this study, we focused on investigating the impact of midbrain dopamine neuron signaling on peripheral immunity. While our approach yielded significant findings, several methodological limitations warrant consideration. First, the viral constructs employed in our study reliably transduced the entire dopaminergic midbrain, encompassing both the substantia nigra pars compacta (SNc) and the ventral tegmental area (VTA). This broad transduction precludes our ability to distinguish the specific contributions of SNc versus VTA neurons to the regulation of the peripheral immune system. Future studies utilizing more refined viral constructs with limited diffusion in the injection region could enable the precise dissection of these distinct neuronal populations in the context of the midbrain-spleen circuit and peripheral immunity are therefore needed. Second, our data suggest that midbrain dopamine neurons send projections throughout the DVC, including AP, NTS, and DMV, preventing us from determining whether a specific nucleus within the DVC contributes predominantly to splenic immunoregulation mediated by midbrain dopamine signaling. Future studies employing targeted inhibition of individual DVC nuclei, such as the NTS, DMV, or AP, during dopamine neuron activation will help delineate the

specific roles of each nucleus in splenic immune modulation. Third, the literature suggests that unilateral vagus nerve stimulation may induce more pronounced changes in the peripheral immune system[104,105]. However, our bilateral approach does not allow us to assess whether the left or right vagal pathway exerts greater influence on midbrain dopamine neuron regulation of splenic immunity. Addressing this limitation in future studies will involve investigating the laterality of midbrain-spleen immunoregulation, which could provide deeper insights into the lateral specificity of this pathway. Such findings could have important implications for experimental designs and therapeutic applications based on these mechanisms. Despite these limitations, our findings represent an important step toward understanding the role of midbrain dopamine signaling in regulating peripheral immunity. By addressing these methodological constraints in future studies, we aim to refine our understanding of the midbrain-DVC-celiac ganglion-spleen pathway and its broader implications for neuroimmunological regulation.

Figure legends

Figure 1. Anterograde neural circuit tracing, showing Midbrain-to-DVC monosynaptic projections. Panel A: Anatomic location of injection of AAV2-DIO-eYFP anterograde tracer into mouse brain expressing cre-recombinase in DAT^+ cells, followed by three-week expression period. **Panel B:** eYFP expression in positive control region median forebrain bundle. **Panel C:** eYFP expression at the injection site in the midbrain. Note also that tyrosine hydroxylase (TH) co-staining confirmed the fidelity of expression in dopaminergic projections from the midbrain in B and C. **Panel D:** The Dorsal Vagal Complex (DVC), as identified by choline acetyltransferase (ChAT) expression in the dorsal motor nucleus of the vagus. **Panel E:** Higher magnification image showing eYFP+ projections surrounding $ChAT^+$ DMV neurons in the DVC, suggesting monosynaptic projections from the midbrain to DVC. *Data representative of N=6 independent experiments.*

Figure 2. Neural circuit tracing data showing that DAT^+ midbrain neurons make synapses throughout the dorsal vagal complex. Panel A: Anatomic locations in brains of DATcre mice receiving midbrain injections of anterograde cre-dependent AAV encoding synaptophysin-mRuby. Three weeks after midbrain injection of monosynaptic anterograde Cre-dependent AAV expressing synaptophysin-mRuby, the resulting fluorescence patterns indicate that midbrain dopamine neurons not only send projections to the DVC but also make synapses in the DVC. **Panel B:** Synaptophysin puncta in control regions of striatum. **Panel C:** Synaptophysin puncta at the injection site in the midbrain. [Panels B and C also show tyrosine hydroxylase (TH) co-staining to confirm expression in dopaminergic projections from the midbrain.] **Panel D:** Presence of mRuby-Synaptophysin puncta throughout DVC, the latter identified by presence of choline acetyl-transferase (ChAT). **Panel E:** Higher magnification of ChAT+ and ChAT-DVC regions showing synaptophysin puncta in both DMV and NTS regions of the DVC, indicating DAT+ midbrain neurons make synapses throughout the DVC. *Data representative of N=6 independent experiments.*

Figure 3. Electrophysiological properties of dorsal vagal complex neurons in response to dopamine indicate presence of D1-like and D2-like receptor expression in the DVC. **Panel A:** GFP-expressing neurons of the Nucleus of the Solitary Tract (NTS) of adult Chat-GFP mice were recorded, using whole-cell patch clamp. Left: Anatomic drawing of brain, showing region of interest. Right: Position of the patching pipette on a GFP-positive neuron from this region. All recordings were performed on coronal slices in the presence of synaptic inhibitors for GABA and Glutamate signaling (see Materials & Methods). **Panel B:** Summary plots of passive properties of GFP-expressing neurons (n = 12) in the NTS, before (i.e., pre-dopamine), black circles, and after (post-dopamine), blue circles, with bath administration of 50 μM dopamine, including group

averages (± S.E.M.), where R_i is the input resistance, and τ (tau) is the membrane time constant. **Panel-C:** Summary plots of active properties of GFP-expressing neurons (n = 12) in the NTS, before (i.e., pre-dopamine), black circles, and after (post-dopamine), blue circles, with bath administration of 50 μM dopamine, including group averages (± S.E.M.). (Note: $I_{threshold}$ is minimal step current to elicit an action potential; $V_{threshold}$ is the membrane voltage threshold to generate an action potential, V_{Height} is the total amplitude of the action potential; $AP_{halfwidth}$ is the width of the first action potential at threshold, measured at half the peak amplitude; SFA ratio us the spike frequency adaptation, measured as the ratio between the second instantaneous frequency and the last of a train of action potentials upon depolarizing currents.) **Panel D:** Example of a putative dopamine D1 receptor expressing cell. **D-1 and D-2**: The neuron was held at –70 mV and subjected to 13 steps of current (from –100 to +500 pA, in 50-pA steps) in the absence (Pre-dopamine: black lines, **D-1**) or after bath administration of 50 μM Dopamine (Post-dopamine: blue lines, **D-2**), showing a decrease in current threshold (*i.e.*, the minimal step of current required to elicit an action potential) and an increase number of action potentials at higher depolarizing currents. **D-3**: quantification of the top panels, showing the firing rate (Hz) of the cell before and after bath administration of 50 μM dopamine as a function of the depolarizing injected current (Pre-dopamine: black line and circles; Post-dopamine: blue line and circles). **D-4**: integration properties of the patched neuron, in response 5 to consecutive 5 msec EPSP-like steps at 20Hz (grey trace, stimulation), showing no difference between the baseline (black trace) and after the administration of dopamine (blue trace). These responses are compatible with the expression of the D1 receptor, which is associated with lower rheobase and membrane threshold, with an overall increase in neuronal excitability. **Panel E:** Example of a putative dopamine D2 receptor expressing cell. **E-1 and E-2**: the neuron was held at –70 mV and subjected to 13 steps of current (from –100 to +500 pA, in 50-pA steps) in the absence or after bath administration of 50 μM Dopamine, showing an increase in current threshold (the minimal step of current required to elicit an action potential) and a decrease number of action potentials at higher depolarizing currents (pre-dopamine: black lines; post-dopamine: blue lines). **E-3**: quantification of the top panels, showing the firing rate (Hz) of the cell before (black line and circles) and after (blue line and circles) bath administration of 50 μM dopamine as a function of the depolarizing injected current. **E-4**: integration properties of the patched neuron, in response 5 to consecutive 5 msec EPSP-like steps at 20Hz (grey trace, stimulation), showing the abolition of synaptic integration properties, after administration of dopamine (blue trace) compared to baseline (black trace). These responses are compatible with the expression of the D2 receptor, which is associated with an overall decrease in neuronal excitability.

Figure 4. Midbrain dopamine neuron projections expressing excitatory DREADD receptors in the DVC release dopamine upon stimulation with CNO, and upon stimulation with methamphetamine, indicating functional projections from midbrain DAT+ neurons to DVC. Panel A: Anatomic midbrain locations of DATcre mice receiving AAV2-DIO-hM3D(Gq)-DREADD-mCherry. In the same surgery, mice received AAV9-hSyn-dLight1.3b in the DVC, followed by expression for 3 weeks. **Panel B:** Coronal sections containing DVC (highlighted in orange) were obtained. **Panel C:** Co-staining for ChAT to identify DVC, DREADD receptor expression in dopamine neuron terminals was verified (data representative of n = 3 biological replicates). **Panel D:** Stimulated release of dopamine from dopamine terminals originating in the midbrain, as indicated in acute coronal sections obtained from parallel cohorts of mice, upon bath perfusion of CNO (10 μM), resulting in a significant increase in dLight1.3b signal. **Panel E:** Additional incremental increase in DA release within the DVC, upon bath perfusion of methamphetamine (10 μM), as determined in separate experiments. **Panel F:** Positive control obtained at 100 μM dopamine, verifying that the observed fluorescent increase was indeed that of the dLight1.3b signal (*N=4 independent biological replicates, with 2 technical replicates per experiment; *p<0.05, two-tailed unpaired Student's T-test*).

Figure 5. Anterograde multi-transsynaptic AAV tracing reveals midbrain-to-spleen connectivity via the celiac ganglion. Panel A: Sagittal view of mouse brain, showing multi-transsynaptic site of midbrain, where Ai9-Flox-stop-TdTomato mice was injected with AAV1-cre. **Panel B:** Diagram showing where, after three weeks of viral expression, the DVC, celiac ganglia and spleen were assessed via confocal microscopy for expression of TdTomato. **Panel C:** IDVC neurons are positive for TdTomato, indicating midbrain-to-DVC projections, in a manner that is consistent with our prior findings. **Panels D and E:** Assessment of celiac ganglia and spleen show presence of TdTomato$^+$ neurons in both organs, indicating both organs received multi-transsynaptic projections from midbrain dopamine neurons. Taken together with our earlier neural circuit tracing data, these findings indicate that multi-synaptic projections exist from midbrain dopamine neurons, via DVC and celiac ganglia, to the spleen. *Data representative of N=4 independent experiments.*

Figure 6. DREADD expression in midbrain dopamine neurons increases cFos expression in the DVC, indicating that dopamine neuron activation can modulate DVC activity. Panel A: Experiment time-line, showing (left) site of cre-dependent Gq DREADD AAV or empty vector injections into the midbrain DATcre mice, (middle-left) four-week expression interval, (middle-right) daily I.P. injections of clozapine-*N*-oxide (1mg/kg), and (right) cFos immunolocalization in DVC as a proxy measure of neuronal activation. **Panel B:** Absence of cFos immunostaining in the mid-brain of mice receiving empty vector. **Panel C:** Robust cFos immunostaining in midbrain of mice treated with AAV encoded with cre-dependent Gq DREADD. **Panel D:** Compared to Empty Vector control, mice receiving Gq DREADD show significantly increased number of cFos+ cells in the DVC. (*Data representative of N=6-7 independent biological replicates; *p<0.05, two-tailed unpaired Student's T-test*)

Figure 7. DREADD stimulation of midbrain dopamine neurons increases cFos expression in celiac ganglia, indicating that dopamine neuron activity can modulate celiac ganglia activity via Midbrain-DVC-celiac ganglion pathway. Panel A: Excitatory Gq DREADDs or empty vector control under control of Cre-recombinase was injected in the midbrain of DATcre mice. After 4 weeks to allow viral expression, mice received 14 days of I.P. CNO (1mg/kg). cFos immunoreactivity was measured as a proxy measure for increased celiac ganglion neuronal activity due to midbrain dopamine neuron activation. **Panel B-C**: Compared to empty vector control, animals that received Gq DREADDs and I.P. CNO show increased celiac ganglion cFos expression. **Panel D**: Mice receiving Gq DREADDs show significantly increased number of cFos+ cells in the celiac ganglion. (*Data representative of N=3-4 independent biological replicates; *p<0.05, two-tailed unpaired Student's T-test*)

Figure 8. Spleen weight and flow cytometric analysis, showing that stimulation of midbrain dopamine neurons by DREADD results in reduced spleen weight and reduced naïve CD4$^+$ T-cell numbers in the spleen without effect on CD8$^+$ T-cells. Panel A: Experiment timeline, showing (left) site of cre-dependent Gq DREADD AAV or empty vector injections into the midbrain DATcre mice, (middle-left) four-week expression interval, followed by daily I.P. injections of clozapine-*N*-oxide (1mg/kg) for two weeks, (middle) harvesting spleen for weighing (middle-right) cellular dissociation, and (right) flow cytometry using antibodies against T-cell subtypes. **Panel B:** Reduced spleen weight, when adjusted for body weight) in mice receiving midbrain Gq DREADD, as compared to empty vector control ($p<0.05$). **Panels C/D**: Single live cells, free of debris, were gated for CD3 expression using a pan-T-cell marker and then gated for expression of CD4 and CD8. **Panels D through G:** CD4$^+$ and CD8$^+$ T-cells were analyzed by expression of CD44 and/or CD62L to assess populations of T-effector memory cells (TEMs), T-central memory cells (TCMs) or naïve T-cells. **Panels H through K:** With no change in total CD4+ T-cell populations, compared

to empty vector control, animals that received Gq excitatory DREADDs in midbrain dopamine neurons show significantly reduced naïve CD4+ T-cells, marked by expression of CD62L and lacking expression of CD44. $CD4^+$ T-effector memory cells and T-central memory cells were not significantly changed. **Panels L through O:** Further evidence that CD8 T-cell subsets are not significantly changed by Gq DREADD midbrain dopamine neuron activation. *(N=4 independent biological replicates; *p<0.05, two-tailed unpaired Student's T-test)*

Supplementary Figure 1. Single channel control images for eYFP-expressing midbrain and median forebrain bundle verify injection site and expression in midbrain dopamine neuron projections. **Panel A:** Median forebrain bundle of DATcre mice injected with DIO-antero-eYFP-AAV2 shows $eYFP^+$ fibers and overlap with TH immunoreactive fibers. **Panel B:** At the midbrain site of injection, $eYFP^+$ cell bodies overlap with TH+ midbrain dopamine neurons.

Supplementary Figure 2. Single channel control images for synaptophysin-expressing midbrain and striatum verify injection site and expression in midbrain dopamine neuron projections. **Panel A:** Striatum of DATcre mice injected with DIO-antero-Synaptophysin-mRuby-AAV shows synaptophysin-mRuby+ terminals and overlap with TH immunoreactive terminals. **Panel B**: At the midbrain site of injection, synaptophysin-mRuby+ cell bodies overlap with TH+ midbrain dopamine neurons.

Supplementary Figure 3. mCherry-tagged Gq DREADDs under control of Cre-recombinase are expressed in midbrain dopamine neurons and terminal regions including the DVC. DATcre mice received midbrain microinjections of Cre-dependent AAV-DIO-mCherry-hM3D (Gq DREADD). mCherry fluorescence was assessed in midbrain and in terminal regions. **Panel A**: Single channel control images show midbrain dopamine neurons, identified by expression of TH, express mCherry-tagged Gq DREADD receptor. **Panel B**: mCherry positive terminals are evident throughout the striatum, indicating this AAV construct expresses Gq DREADD receptors in terminal regions. **Panel C**: mCherry+ Gq DREADD expressing terminals are evident throughout the DVC.

Supplementary Figure 4: Gq DREADD stimulation of midbrain dopamine neurons increases cFos expression in both midbrain and striatum. DATcre mice received midbrain microinjections of AAV-DIO-mCherry-hM3D (Gq DREADD). Panel A-C: Midbrain dopamine neurons of mice that received excitatory Gq DREADDs, identified by expression of DAT, show robust cFos expression following systemic CNO administration. Panel D-F: Striatal terminal regions of dopamine neurons, identified by DAT expression, also exhibit robust cFos expression.

Supplementary Figure 5: Gq DREADD stimulation results in increased locomotor activity following intraperitoneal injection of 1mg/kg clozapine-*N*-oxide. Panel A: Locomotor activity in the home cage was measured prior to drug injection (Day 0), and on Days 1, 7 and 13 during the CNO administration period. **Panel B:** On Day 0, total distance traveled is not significantly different between animals receiving Gq DREADD in midbrain dopamine neurons relative to empty vector control. Consistent with the literature in the field, CNO increases locomotor activity in animals with midbrain dopamine neuron Gq DREADDs compared to empty vector on Days 1, 7 and 13. **Panel C:** Average speed is also significantly increased in animals receiving Gq DREADDs relative to empty vector control on Days 1, 7 and 13. See also Supplementary Movie 1.

Supplementary Figure 6. Fluorescence-minus-one generated gating strategy to analyze splenic T-cell populations. **Panel A**: Single, live cells free of debris were (**Panel B**) assessed for expression of CD45. **Panel B**: Subsequently, cells expressing CD3 were assessed for CD4 and CD8 expression, and then assessed for T-central memory (TCM), T-effector memory (TEM)

and Naïve T-cells. **Panels C-H**: Gates for analyses for each of the above populations were set by fluorescence-minus-one gating strategy.

Supplementary Figure 6. Plasma corticosterone levels are not changed in mice receiving midbrain Gq DREADDs compared to empty vector control.

Supplementary Video 1: Increased locomotor activity evident throughout 14 days of systemic CNO treatment in mice that received excitatory Gq DREADD AAV injection in midbrain dopamine neurons.

Materials and Methods:

Animals

We used the following strains of mice on a C57/B6 background: Ai9 (strain #007909), DAT:cre (strain #020080), ChAT-GFP (strain #007902). Adult male and female mice were between 8-16 weeks of age, on a 12 hour day/night cycle with ad libitum access to food and water. Animals were bred in house at the University of Florida or at the University of Texas San Antonio, following approved procedures by the University of Florida IACUC (IACUC 20240000184) or by the University of Texas San Antonio IACUC (IACUC MU096).

Stereotactic surgeries and viral injections

Mice were anesthetized using gas anesthetic (3% isoflurane mixed with oxygen) via a certified veterinary vaporizer. After head shaving, mice were head fixed in a stereotactic frame (Kopf Instruments). Following sterilization of the surgical site using alternating scrubs of chlorhexidine and sterile saline, an incision was made, skull exposed and leveled from bregma to lambda, and burr holes drilled at the surgical coordinates (Bregma: +0.4ML, -3.4AP, -4.4DV). Virus was injected at a rate of 5nL every 5 seconds, until injection was complete (Drummond Nanoject III). Injector was left in place for 5 minutes to allow spread prior to retraction. Scalp skin was sutured using 3 interrupted sutures (5.0 polypropylene sutures). Virus was allowed to express for 3 weeks prior to experiments. Viral vectors given in **Table 1**.

Electrophysiology

As described in previous studies (Rock & Apicella, 2015; Rock et al., 2016a; Zurita et al., 2017; Rock et al., 2018; Zurita et al., 2018a; Bertero et al., 2020; Bertero et al., 2021, Bertero et al., 2024), after 3-4 weeks from the viral injection, mice were anesthetized with isoflurane and decapitated. Coronal slices (300 µm) containing the DVC, based on neuroanatomical landmarks, of interest were obtained on a vibratome (VT1200S, Leica) in a chilled cutting solution containing 100 mM choline chloride, 25 mM $NaHCO_3$, 25 mM D-glucose, 11.6 mM sodium ascorbate, 7 mM $MgSO_4$ 3.1 mM sodium pyruvate, 2.5 mM KCl, 1.25 mM NaH_2PO_4, 0.5 mM $CaCl_2$. Slices were then incubated in oxygenated artificial cerebrospinal fluid (ACSF) in a sub-merged chamber at 35–37°C for 30 min and then at room temperature (21–25°C), until recordings were performed. ACSF contained 126 mM NaCl, 26 mM $NaHCO_3$, 10 mM D-glucose, 2.5 mM KCl, 2 mM $CaCl_2$, 1.25 mM NaH_2PO_4, 1 mM $MgCl_2$; osmolarity was ~290 Osm/L.

Whole-cell recordings were performed in 31–33°C artificial cerebrospinal fluid (ACSF). Thin-walled borosilicate glass pipettes (Warner Instruments) were pulled on a vertical pipette puller (PC-10, Narishige), resulting in a typical range of 3–5 MΩ resistance. ChAT+ GFP-expressing neurons were identified to locate the DVC, and intrinsic properties were recorded in the current-clamp configuration using a potassium-based intracellular solution which contained 120 mM potassium gluconate, 20 mM KCl, 10 mM HEPES, 10 mM phosphocreatine, 4 mM ATP, 0.3 mM GTP, 0.2 mM EGTA, and 0.3–0.5% biocytin (mg/mL)). Signals were sampled at 10 kHz

and filtered (lowpass filter) at 4 kHz., in the presence of excitation and inhibition blockers. Pharmacological blockers used were as follows: CPP (5 μM; Tocris Bioscience), NBQX (10 μM; Abcam), and gabazine (25 μM; Abcam). Hardware control and data acquisition were performed with the Matlab-based Ephus package (Suter et al., 2010). The resting membrane potential (Vm) was calculated in current clamp mode (I = 0) immediately after breaking in. Series (R_s) and input resistance (R_{in}) were calculated in voltage-clamp mode (V_{hold} = −70 mV) by giving a −5 mV step, which resulted in transient current responses. R_s was determined by dividing the voltage step amplitude by the peak of the capacitive current generated by the voltage step. The difference between baseline and steady-state hyperpolarized current (ΔI) was used to calculate Rin using the following formula: $R_{in} = -5\ mV/\Delta I - R_s$. Subthreshold and suprathreshold membrane responses in current-clamp were elicited by injecting −100 to +500 pA in 50-pA increments at V_{hold} = −70 mV. The first resulting AP at rheobase (the minimal current of infinite duration - experimentally limited to 1 s, as required to generate an AP, from here on current threshold, or I threshold) was analyzed for AP width, peak, height, Voltage threshold. The adaptation ratio was measured at the current step that gave the closest APs firing rate to 20 Hz, calculated dividing the second instantaneous frequency by the last. The f/I graphs were generated by calculating the firing frequency at each positive current step administered to the cell while holding the cell at -70 mV. Alpha synapse was calculated by measuring the peak of five consecutive 5 msec EPSP-like steps at 20Hz and normalizing the amplitude of the first peak.

Ex vivo dLight1.3b recording

Preparation of acute midbrain slices: The mice were perfused with ice cold sucrose-sodium-replacement solution containin 250 mM sucrose, 26 mM $NaHCO_3$, 2 mM KCl, 1.2 mM NaH_2PO_4, 11 mM dextrose, 7 mM $MgCl_2$, and 0.5 mM $CaCl_2$. Mice were decapitated, their brains were promptly removed. For slicing, the brain was cut rostrally to the cerebellum in the coronal plane to create a flat surface for attachment to the cutting stage. Coronal brainstem sections containing the dorsal vagal complex (DVC) were sectioned at 250μm (VT1200, Leica). The slices were transferred to a recovery chamber containing oxygenated artificial cerebrospinal fluid (ACSF) at 34C. The ACSF composition included: 126 mM NaCl, 2.5 mM KCl, 2 mM $CaCl_2$, 26 mM $NaHCO_3$, 1.25 mM NaH_2PO_4, 2 mM $MgSO_4$, and 10 dextrose, equilibrated with 95% O_2 and 5% CO_2. The osmolarity for both the sucorse-sodium-replacement and ACSF was adjusted to 300-310 mOsm and the pH was set to 7.35-7.4. Sections remained in the recovery chamber for at least 30 minutes at 34C until used for subsequent ex-vivo dLight1.3b recording.

Recording: The slices were then transferred to a low-profile open diamond bath imaging chamber (RC-26GLP, Warner Instruments, Hamden, CT, USA) and perfused with ACSF at 36-37°C. Sections were imaged using a 40x water-immersion objective on an Eclipse FN1 upright microscope (Nikon Instruments, Inc., Melville, NY, USA). The microscope was equipped with a Spectra X light engine (Lumencor, Beaverton, OR, USA) and a 470/24 nm solid-state illumination source. Images were captured with a Hamamatsu BT Fusion camera (Hamamatsu). Gq DREADD receptors were activated via bath perfusion of 10uM clozapine-N-oxide (CNO) in ACSF.

Signal bleach correction: Raw fluorescent intensity values were extracted using ImageJ. A photobleaching curve was generated by fitting the baseline florescent signal using a non-linear least regression with a biexponential model. Traces were then corrected and normalized using MATLAB.

Dissection of the sympathetic splanchnic-celiac-superior mesenteric ganglion complex (SCSMG)

Mice were deeply anesthetized with isoflurane, and transcardiac perfused with PBS, followed by 4% paraformaldehyde (PFA). The sympathetic ganglion complex was dissected following Trevizan-Baú et al. (2024)[46]. Briefly, mice were positioned in dorsal recumbency, and the abdominal wall was opened (in the Linea Alba). With fine forceps and Noyes Iris scissors, the

sympathetic ganglion complex was dissected and collected under a stereo microscope. The complex was then placed onto a Sylgard coated dissection dish with PBS and pinned down on the dish through connective tissue and nerves, not through the ganglia. Then, after removing any additional connective tissue or fat, the sympathetic ganglion complex was post-fixed for 24 hours before using for immunostaining and imaging.

Brain Tissue and Spleen immunofluorescence and imaging

Animals were terminally anesthetized with isoflurane, and transcardiac perfused with 1x PBS followed by 4% PFA dissolved in PBS (pH 7.4). Brains were removed and post-fixed in 4% PFA for 24 hours at 4 degrees C. Spleens were removed prior to perfusion and post-fixed in 4% PFA for 24 hours at 4C. Thereafter, sections were cut at 40um thickness at room temperature on a vibrating microtome (Leica VT1000). Free-floating sections were blocked at 37 degrees C for 1 hour in 0.3% Triton X-100 in PBS, containing 5% normal goat serum or fetal bovine serum. The slices were incubated with primary antibody overnight in 0.3% TritonX-100 in PBS, containing 5% normal goat serum or fetal bovine serum. Following washes, slices were incubated with corresponding fluorophore-conjugated secondaries for 1 hour at room temperature, washed and mounted (Fluoromount, Invitrogen). Antibodies and concentrations are given in **Table 2**.

Flow cytometry

Following terminal isofluorane anesthesia, the spleen was removed and placed in PBS on ice. Sterile tissue forceps were used to remove the spleen, placed on a slide and disrupted to produce a splenocyte suspension. Slides were washed using 3 volumes of PBS to collect splenocyte suspension, followed by filtration through a 40 µm cell strainer placed over a 50mL conical tube. Following centrifugation (300 x g, 5 min), cell pellet was resuspended in 70% Percoll density medium, and then underlaid below 37% Percoll. Centrifugation for 30 min at 500 x g with brakes and acceleration set to low results in a suspension of splenocytes at the interface between 37% and 70% Percoll. Cells were collected, washed twice with excess PBS, and then counted and density adjusted to 10,000 cells per microliter. Flow cytometry staining was conducted using 1 million cells suspended in 100uL of PBS. Antibodies and concentrations are given in **Table 3**.

Table 1: Adeno-Associated Viruses

AAV	Purpose	Vendor	Catalog #	Concentration	Volume injected
AAV2-Ef1a-DIO-EYFP	Tracing	Addgene	27056	$1x10^{13}$ vg/mL	200nL
AAV1-hSyn-Flex mGFP-2A-Synaptophysin-mRuby	Tracing	Addgene	71760	$7x10^{12}$ vg/mL	100nL
pENN-AAV1-hSyn-Cre-WPRE-hGH	Tracing	Addgene	105553	$7x10^{12}$ vg/mL	100nL
AAV9-syn-dLight1.3b	Dopamine sensor	Addgene	135762	$1x10^{13}$ vg/mL	50nL
AAV2-hSyn-DIO-	Excitatory DREADD	Addgene	44361	$6x10^{12}$ vg/mL	200nL

hM3D(Gq)-mCherry					
AAV2-hSyn-DIO-mCherry	Empty Vector control	Addgene	50459	$6x10^{12}$ vg/mL	200nL

Table 2: Antibodies for immunofluorescence

Specificity	Clone/Species	Conjugate	Vendor	Catalog Number	Purpose	Dilution
DAT	Polyclonal/Rat	N/A	EMD Millipore Corp.	MAB369	IHC	1:500
TH	Polyclonal/Rabbit Polyclonal/Chicken	N/A	Encor	RPCA-TH CPCA-TH	IHC	1:500
CD3	Polyclonal/Rat	N/A	BioLegend	100201	IHC	1:1000
IBA1	Monoclonal/Guinea Pig	N/A	Synaptic Systems	234308	IHC	1:500
ChAT	Polyclonal/Goat	N/A	EMD Millipore Corp.	AB144P	IHC	1:200
Anti-GFP	Monoclonal/Mouse	N/A	Invitrogen	A11122	IHC	1:500
mCherry	Polyclonal/Mouse	N/A	Encor	MPCA-mCherry	IHC	1:500
cFos	Polyclonal/Rabbit	N/A	Encor	RPCA-c-FOS	IHC	1:500
B220	Polyclonal/Rat	N/A	BioLegend	103202	IHC	1:500
Rat	Polyclonal/Goat	Alexafluor-488 Alexafluor-647	Invitrogen	A11006 A21247	IHC	1:500
Rabbit	Polyclonal/Goat	Alexafluor-488 Alexafluor-568	Invitrogen	A11034 A11011	IHC	1:500
Guinea Pig	Polyclonal/Goat	Alexafluor-488	Invitrogen	A11073	IHC	1:500
Mouse	Polyclonal/Goat	Alexafluor-647	Invitrogen	A21236	IHC	1:500
Chicken	IgY	Alexafluor-647	Invitrogen	A21449	IHC	1:1000
Goat	Polyclonal/Donkey	Alexafluor-647	Invitrogen	A21447	IHC	1:500

Table 3: Antibodies for Flow Cytometry

Specificity	Clone/Species	Conjugate	Vendor	Catalog #	Purpose	Dilution (Spleen)
CD3	17A2/Rat	Pac Blue	BioLegend	100214	FC	1:50
CD4	GK1.5/Rat	AF700	BioLegend	100430	FC	1:100
CD8a	QA17A07/Mouse	Spark 538	BioLegend	155020	FC	1:50
CD127	S18006K/Rat	PE/Fire 640	BioLegend	158213	FC	1:100
CD45	30-F11/Rat	Spark Blue 574	BioLegend	103184	FC	1:200
CD44	IM7/Rat	Spark Yg 594	BioLegend	103078	FC	1:100
CD62L	MEL-14/Rat	BV711	BioLegend	104445	FC	1:200

Acknowledgements: We acknowledge assistance from Leah T. Phan, Emily J. Miller, and Kaitlyn N. Kiel. In addition, we acknowledge technical assistance from the University of Florida Center for Immunology and Transplantation.

References

1 Jin, H., Li, M., Jeong, E., Castro-Martinez, F. & Zuker, C. S. A body–brain circuit that regulates body inflammatory responses. *Nature* **630**, 695-703, doi:10.1038/s41586-024-07469-y (2024).

2 Zhu, X. *et al.* Somatosensory cortex and central amygdala regulate neuropathic pain-mediated peripheral immune response via vagal projections to the spleen. *Nature Neuroscience* **27**, 471-483, doi:10.1038/s41593-023-01561-8 (2024).

3 Tansey, M. G. *et al.* Inflammation and immune dysfunction in Parkinson disease. *Nat Rev Immunol* **22**, 657-673, doi:10.1038/s41577-022-00684-6 (2022).

4 Cossu, D., Hatano, T. & Hattori, N. The Role of Immune Dysfunction in Parkinson's Disease Development. *Int J Mol Sci* **24**, doi:10.3390/ijms242316766 (2023).

5 Tan, E. K. *et al.* Parkinson disease and the immune system - associations, mechanisms and therapeutics. *Nat Rev Neurol* **16**, 303-318, doi:10.1038/s41582-020-0344-4 (2020).

6 Gopinath, A. *et al.* Methamphetamine induces a low dopamine transporter expressing state without altering the total number of peripheral immune cells. *Basic Clin Pharmacol Toxicol* **133**, 496-507, doi:10.1111/bcpt.13838 (2023).

7 Weaver, J. L. *et al.* Methamphetamine Use is Associated with Increased Surgical Site Infections after Trauma Laparotomy. *J Surg Res* **267**, 563-567, doi:10.1016/j.jss.2021.06.034 (2021).

8 Hulsebos, I. F. *et al.* Stimulant Abuse in Burn Patients Is Associated With an Increased Use of Hospital Resources. *J Burn Care Res* **41**, 921-925, doi:10.1093/jbcr/iraa087 (2020).

9 Salamanca, S. A., Sorrentino, E. E., Nosanchuk, J. D. & Martinez, L. R. Impact of methamphetamine on infection and immunity. *Front Neurosci* **8**, 445, doi:10.3389/fnins.2014.00445 (2014).

10 Eisenberger, N. I. *et al.* Inflammation-induced anhedonia: endotoxin reduces ventral striatum responses to reward. *Biol Psychiatry* **68**, 748-754, doi:10.1016/j.biopsych.2010.06.010 (2010).
11 Lee, Y. *et al.* Anti-cytokine agents for anhedonia: targeting inflammation and the immune system to treat dimensional disturbances in depression. *Ther Adv Psychopharmacol* **8**, 337-348, doi:10.1177/2045125318791944 (2018).
12 Mehta, N. D. *et al.* Inflammation, reward circuitry and symptoms of anhedonia and PTSD in trauma-exposed women. *Soc Cogn Affect Neurosci* **15**, 1046-1055, doi:10.1093/scan/nsz100 (2020).
13 Cooper, C. M., Farrand, A. Q., Andresen, M. C. & Beaumont, E. Vagus nerve stimulation activates nucleus of solitary tract neurons via supramedullary pathways. *J Physiol* **599**, 5261-5279, doi:10.1113/jp282064 (2021).
14 Jayaprakash, N. *et al.* Organ- and function-specific anatomical organization of vagal fibers supports fascicular vagus nerve stimulation. *Brain Stimul* **16**, 484-506, doi:10.1016/j.brs.2023.02.003 (2023).
15 Matteoli, G. & Boeckxstaens, G. E. The vagal innervation of the gut and immune homeostasis. *Gut* **62**, 1214, doi:10.1136/gutjnl-2012-302550 (2013).
16 Pavlov, V. A. & Tracey, K. J. The cholinergic anti-inflammatory pathway. *Brain Behav Immun* **19**, 493-499, doi:10.1016/j.bbi.2005.03.015 (2005).
17 Alen, N. V. The cholinergic anti-inflammatory pathway in humans: State-of-the-art review and future directions. *Neurosci Biobehav Rev* **136**, 104622, doi:10.1016/j.neubiorev.2022.104622 (2022).
18 Wu, S. J. *et al.* Activation of the Cholinergic Anti-inflammatory Pathway Attenuated Angiotension II-Dependent Hypertension and Renal Injury. *Front Pharmacol* **12**, 593682, doi:10.3389/fphar.2021.593682 (2021).
19 Rosas-Ballina, M. *et al.* Splenic nerve is required for cholinergic antiinflammatory pathway control of TNF in endotoxemia. *Proc Natl Acad Sci U S A* **105**, 11008-11013, doi:10.1073/pnas.0803237105 (2008).
20 Huston, J. M. *et al.* Cholinergic neural signals to the spleen down-regulate leukocyte trafficking via CD11b. *J Immunol* **183**, 552-559, doi:10.4049/jimmunol.0802684 (2009).
21 Leaders, F. E. & Dayrit, C. THE CHOLINERGIC COMPONENT IN THE SYMPATHETIC INNERVATION TO THE SPLEEN. *J Pharmacol Exp Ther* **147**, 145-152 (1965).
22 Vida, G., Peña, G., Deitch, E. A. & Ulloa, L. α7-cholinergic receptor mediates vagal induction of splenic norepinephrine. *J Immunol* **186**, 4340-4346, doi:10.4049/jimmunol.1003722 (2011).
23 Mota, C. M. D. & Madden, C. J. Neural control of the spleen as an effector of immune responses to inflammation: mechanisms and treatments. *Am J Physiol Regul Integr Comp Physiol* **323**, R375-r384, doi:10.1152/ajpregu.00151.2022 (2022).
24 Bellinger, D. L., Felten, S. Y., Lorton, D. & Felten, D. L. Origin of noradrenergic innervation of the spleen in rats. *Brain Behav Immun* **3**, 291-311, doi:10.1016/0889-1591(89)90029-9 (1989).
25 Wu, M. *et al.* Innervation of nociceptor neurons in the spleen promotes germinal center responses and humoral immunity. *Cell* **187**, 2935-2951.e2919, doi:10.1016/j.cell.2024.04.027 (2024).

26 Han, W. *et al.* A Neural Circuit for Gut-Induced Reward. *Cell* **175**, 665-678.e623, doi:10.1016/j.cell.2018.08.049 (2018).
27 Marvel, F. A., Chen, C. C., Badr, N., Gaykema, R. P. & Goehler, L. E. Reversible inactivation of the dorsal vagal complex blocks lipopolysaccharide-induced social withdrawal and c-Fos expression in central autonomic nuclei. *Brain Behav Immun* **18**, 123-134, doi:10.1016/j.bbi.2003.09.004 (2004).
28 Chavan, S. S., Pavlov, V. A. & Tracey, K. J. Mechanisms and Therapeutic Relevance of Neuro-immune Communication. *Immunity* **46**, 927-942, doi:10.1016/j.immuni.2017.06.008 (2017).
29 Zhuang, X., Masson, J., Gingrich, J. A., Rayport, S. & Hen, R. Targeted gene expression in dopamine and serotonin neurons of the mouse brain. *J Neurosci Methods* **143**, 27-32, doi:10.1016/j.jneumeth.2004.09.020 (2005).
30 Beier, K. T. *et al.* Circuit Architecture of VTA Dopamine Neurons Revealed by Systematic Input-Output Mapping. *Cell* **162**, 622-634, doi:10.1016/j.cell.2015.07.015 (2015).
31 Roth, B. L. DREADDs for Neuroscientists. *Neuron* **89**, 683-694, doi:10.1016/j.neuron.2016.01.040 (2016).
32 Van Den Herrewegen, Y. *et al.* Side-by-side comparison of the effects of Gq- and Gi-DREADD-mediated astrocyte modulation on intracellular calcium dynamics and synaptic plasticity in the hippocampal CA1. *Mol Brain* **14**, 144, doi:10.1186/s13041-021-00856-w (2021).
33 Pati, S. *et al.* Chemogenetic Activation of Excitatory Neurons Alters Hippocampal Neurotransmission in a Dose-Dependent Manner. *eNeuro* **6**, doi:10.1523/eneuro.0124-19.2019 (2019).
34 Patriarchi, T. *et al.* An expanded palette of dopamine sensors for multiplex imaging in vivo. *Nat Methods* **17**, 1147-1155, doi:10.1038/s41592-020-0936-3 (2020).
35 Yorgason, J. T. *et al.* Methamphetamine increases dopamine release in the nucleus accumbens through calcium-dependent processes. *Psychopharmacology (Berl)* **237**, 1317-1330, doi:10.1007/s00213-020-05459-2 (2020).
36 Goodwin, J. S. *et al.* Amphetamine and methamphetamine differentially affect dopamine transporters in vitro and in vivo. *J Biol Chem* **284**, 2978-2989, doi:10.1074/jbc.M805298200 (2009).
37 Sambo, D. O. *et al.* The sigma-1 receptor modulates methamphetamine dysregulation of dopamine neurotransmission. *Nat Commun* **8**, 2228, doi:10.1038/s41467-017-02087-x (2017).
38 Pavlov, V. A., Chavan, S. S. & Tracey, K. J. Molecular and Functional Neuroscience in Immunity. *Annu Rev Immunol* **36**, 783-812, doi:10.1146/annurev-immunol-042617-053158 (2018).
39 Hoover, D. B. Cholinergic modulation of the immune system presents new approaches for treating inflammation. *Pharmacol Ther* **179**, 1-16, doi:10.1016/j.pharmthera.2017.05.002 (2017).
40 Kaestner, C. L., Smith, E. H., Peirce, S. G. & Hoover, D. B. Immunohistochemical analysis of the mouse celiac ganglion: An integrative relay station of the peripheral nervous system. *J Comp Neurol* **527**, 2742-2760, doi:10.1002/cne.24705 (2019).

41 Klein Wolterink, R. G. J., Wu, G. S., Chiu, I. M. & Veiga-Fernandes, H. Neuroimmune Interactions in Peripheral Organs. *Annu Rev Neurosci* **45**, 339-360, doi:10.1146/annurev-neuro-111020-105359 (2022).
42 Wang, T., Teng, B., Yao, D. R., Gao, W. & Oka, Y. Organ-specific Sympathetic Innervation Defines Visceral Functions. *bioRxiv*, 2024.2009.2019.613934, doi:10.1101/2024.09.19.613934 (2024).
43 Kressel, A. M. *et al.* Identification of a brainstem locus that inhibits tumor necrosis factor. *Proc Natl Acad Sci U S A* **117**, 29803-29810, doi:10.1073/pnas.2008213117 (2020).
44 Carnevale, D. *et al.* A cholinergic-sympathetic pathway primes immunity in hypertension and mediates brain-to-spleen communication. *Nat Commun* **7**, 13035, doi:10.1038/ncomms13035 (2016).
45 Shinohara, K. Celiac ganglia: potential new targets in neuromodulation for hypertension. *Hypertension Research* **46**, 2235-2236, doi:10.1038/s41440-023-01355-2 (2023).
46 Trevizan-Baú, P. *et al.* Protocol for the isolation of the mouse sympathetic splanchnic-celiac-superior mesenteric ganglion complex. *STAR Protoc* **5**, 103036, doi:10.1016/j.xpro.2024.103036 (2024).
47 Ben-Shaanan, T. L. *et al.* Activation of the reward system boosts innate and adaptive immunity. *Nat Med* **22**, 940-944, doi:10.1038/nm.4133 (2016).
48 Ben-Shaanan, T. L. *et al.* Modulation of anti-tumor immunity by the brain's reward system. *Nat Commun* **9**, 2723, doi:10.1038/s41467-018-05283-5 (2018).
49 Fernandez, R. *et al.* Neural reflex regulation of systemic inflammation: potential new targets for sepsis therapy. *Front Physiol* **5**, 489, doi:10.3389/fphys.2014.00489 (2014).
50 Browning, K. N. & Travagli, R. A. Central nervous system control of gastrointestinal motility and secretion and modulation of gastrointestinal functions. *Compr Physiol* **4**, 1339-1368, doi:10.1002/cphy.c130055 (2014).
51 Martelli, D., Yao, S. T., McKinley, M. J. & McAllen, R. M. Reflex control of inflammation by sympathetic nerves, not the vagus. *J Physiol* **592**, 1677-1686, doi:10.1113/jphysiol.2013.268573 (2014).
52 McAllen, R. M., McKinley, M. J. & Martelli, D. Reflex regulation of systemic inflammation by the autonomic nervous system. *Autonomic Neuroscience* **237**, 102926, doi:https://doi.org/10.1016/j.autneu.2021.102926 (2022).
53 Morgan, J. I., Cohen, D. R., Hempstead, J. L. & Curran, T. Mapping patterns of c-fos expression in the central nervous system after seizure. *Science* **237**, 192-197, doi:10.1126/science.3037702 (1987).
54 Barros, V. N. *et al.* The pattern of c-Fos expression and its refractory period in the brain of rats and monkeys. *Front Cell Neurosci* **9**, 72, doi:10.3389/fncel.2015.00072 (2015).
55 Gao, Y. J. & Ji, R. R. c-Fos and pERK, which is a better marker for neuronal activation and central sensitization after noxious stimulation and tissue injury? *Open Pain J* **2**, 11-17, doi:10.2174/1876386300902010011 (2009).
56 Cullinan, W. E., Herman, J. P., Battaglia, D. F., Akil, H. & Watson, S. J. Pattern and time course of immediate early gene expression in rat brain following acute stress. *Neuroscience* **64**, 477-505, doi:10.1016/0306-4522(94)00355-9 (1995).
57 Lewis, S. M., Williams, A. & Eisenbarth, S. C. Structure and function of the immune system in the spleen. *Sci Immunol* **4**, doi:10.1126/sciimmunol.aau6085 (2019).

58 Wluka, A. & Olszewski, W. L. Innate and adaptive processes in the spleen. *Ann Transplant* **11**, 22-29 (2006).
59 Ugel, S. *et al.* Immune tolerance to tumor antigens occurs in a specialized environment of the spleen. *Cell Rep* **2**, 628-639, doi:10.1016/j.celrep.2012.08.006 (2012).
60 Bronte, V. & Pittet, M. J. The spleen in local and systemic regulation of immunity. *Immunity* **39**, 806-818, doi:10.1016/j.immuni.2013.10.010 (2013).
61 Mebius, R. E. & Kraal, G. Structure and function of the spleen. *Nat Rev Immunol* **5**, 606-616, doi:10.1038/nri1669 (2005).
62 Wu, C., Hua, Q. & Zheng, L. Generation of Myeloid Cells in Cancer: The Spleen Matters. *Front Immunol* **11**, 1126, doi:10.3389/fimmu.2020.01126 (2020).
63 Beheshti, A. *et al.* Tumor-host signaling interaction reveals a systemic, age-dependent splenic immune influence on tumor development. *Oncotarget* **6**, 35419-35432, doi:10.18632/oncotarget.6214 (2015).
64 Markel, J. E. *et al.* Using the Spleen as an In Vivo Systemic Immune Barometer Alongside Osteosarcoma Disease Progression and Immunotherapy with α-PD-L1. *Sarcoma* **2018**, 8694397, doi:10.1155/2018/8694397 (2018).
65 Chen, X. *et al.* Evidence for Peripheral Immune Activation in Parkinson's Disease. *Front Aging Neurosci* **13**, 617370, doi:10.3389/fnagi.2021.617370 (2021).
66 Ghanta, M. K. *et al.* Role of CD4+ T Cells in Parkinson's Disease. *Crit Rev Immunol* **42**, 17-25, doi:10.1615/CritRevImmunol.2023047372 (2022).
67 Mamula, D., Khosousi, S., He, Y., Lazarevic, V. & Svenningsson, P. Impaired migratory phenotype of CD4(+) T cells in Parkinson's disease. *NPJ Parkinsons Dis* **8**, 171, doi:10.1038/s41531-022-00438-0 (2022).
68 Bravo, J., Magalhães, C., Andrade, E. B., Magalhães, A. & Summavielle, T. The impact of psychostimulants on central and peripheral neuro-immune regulation: a scoping review of cytokine profiles and their implications for addiction. *Front Cell Neurosci* **17**, 1109611, doi:10.3389/fncel.2023.1109611 (2023).
69 Carrico, A. W. *et al.* Stimulant use is associated with immune activation and depleted tryptophan among HIV-positive persons on anti-retroviral therapy. *Brain Behav Immun* **22**, 1257-1262, doi:10.1016/j.bbi.2008.07.010 (2008).
70 Glac, W. *et al.* Prolonged Peripheral Immunosuppressive Responses as Consequences of Random Amphetamine Treatment, Amphetamine Withdrawal and Subsequent Amphetamine Challenges in Rats. *J Neuroimmune Pharmacol* **16**, 870-887, doi:10.1007/s11481-021-09988-1 (2021).
71 Wu, H. *et al.* Dynamic immune and exosome transcriptomic responses in patients undergoing psychostimulant methamphetamine withdrawal. *Front Cell Neurosci* **16**, 961131, doi:10.3389/fncel.2022.961131 (2022).
72 Assis, M. A., Hansen, C., Lux-Lantos, V. & Cancela, L. M. Sensitization to amphetamine occurs simultaneously at immune level and in met-enkephalin of the nucleus accumbens and spleen: an involved NMDA glutamatergic mechanism. *Brain Behav Immun* **23**, 464-473, doi:10.1016/j.bbi.2009.01.003 (2009).
73 Gopinath, A. *et al.* DAT and TH expression marks human Parkinson's disease in peripheral immune cells. *NPJ Parkinsons Dis* **8**, 72, doi:10.1038/s41531-022-00333-8 (2022).

74 Gopinath, A. *et al.* Who Knew? Dopamine Transporter Activity Is Critical in Innate and Adaptive Immune Responses. *Cells* **12**, doi:10.3390/cells12020269 (2023).
75 Kavelaars, A., Cobelens, P. M., Teunis, M. A. & Heijnen, C. J. Changes in innate and acquired immune responses in mice with targeted deletion of the dopamine transporter gene. *J Neuroimmunol* **161**, 162-168, doi:10.1016/j.jneuroim.2005.01.004 (2005).
76 Bencsics, A. *et al.* Dopamine, as well as norepinephrine, is a link between noradrenergic nerve terminals and splenocytes. *Brain Res* **761**, 236-243, doi:10.1016/s0006-8993(97)00313-2 (1997).
77 Cano, G., Sved, A. F., Rinaman, L., Rabin, B. S. & Card, J. P. Characterization of the central nervous system innervation of the rat spleen using viral transneuronal tracing. *J Comp Neurol* **439**, 1-18, doi:10.1002/cne.1331 (2001).
78 Murray, K. *et al.* Neuroanatomy of the spleen: Mapping the relationship between sympathetic neurons and lymphocytes. *PLoS One* **12**, e0182416, doi:10.1371/journal.pone.0182416 (2017).
79 Elenkov, I. J., Wilder, R. L., Chrousos, G. P. & Vizi, E. S. The sympathetic nerve--an integrative interface between two supersystems: the brain and the immune system. *Pharmacol Rev* **52**, 595-638 (2000).
80 Ludwig, M. Q. *et al.* A genetic map of the mouse dorsal vagal complex and its role in obesity. *Nat Metab* **3**, 530-545, doi:10.1038/s42255-021-00363-1 (2021).
81 Kim, K. S., Seeley, R. J. & Sandoval, D. A. Signalling from the periphery to the brain that regulates energy homeostasis. *Nat Rev Neurosci* **19**, 185-196, doi:10.1038/nrn.2018.8 (2018).
82 Luquet, S. & Magnan, C. The central nervous system at the core of the regulation of energy homeostasis. *Front Biosci (Schol Ed)* **1**, 448-465, doi:10.2741/s37 (2009).
83 Prinz, M. & Priller, J. The role of peripheral immune cells in the CNS in steady state and disease. *Nat Neurosci* **20**, 136-144, doi:10.1038/nn.4475 (2017).
84 Vaccarino, V. *et al.* Brain-heart connections in stress and cardiovascular disease: Implications for the cardiac patient. *Atherosclerosis* **328**, 74-82, doi:10.1016/j.atherosclerosis.2021.05.020 (2021).
85 Liu, W. *et al.* Brain-heart communication in health and diseases. *Brain Res Bull* **183**, 27-37, doi:10.1016/j.brainresbull.2022.02.012 (2022).
86 Braun, J. *et al.* Central stress pathways in the development of cardiovascular disease. *Clin Auton Res* **34**, 99-116, doi:10.1007/s10286-023-01008-x (2024).
87 Zouridis, S., Nasir, A. B., Aspichueta, P. & Syn, W. K. The Link between Metabolic Syndrome and the Brain. *Digestion*, 1-9, doi:10.1159/000541696 (2024).
88 Petersen, M. *et al.* A latent clinical-anatomical dimension relating metabolic syndrome to brain structure and cognition. *Elife* **12**, doi:10.7554/eLife.93246 (2024).
89 Buchanan, J. B., Sparkman, N. L. & Johnson, R. W. Methamphetamine sensitization attenuates the febrile and neuroinflammatory response to a subsequent peripheral immune stimulus. *Brain Behav Immun* **24**, 502-511, doi:10.1016/j.bbi.2009.12.008 (2010).
90 Kustrimovic, N., Marino, F. & Cosentino, M. Peripheral Immunity, Immunoaging and Neuroinflammation in Parkinson's Disease. *Curr Med Chem* **26**, 3719-3753, doi:10.2174/0929867325666181009161048 (2019).

91 Muñoz-Delgado, L. *et al.* Peripheral inflammatory immune response differs among sporadic and familial Parkinson's disease. *NPJ Parkinsons Dis* **9**, 12, doi:10.1038/s41531-023-00457-5 (2023).
92 Lucido, M. J. *et al.* Aiding and Abetting Anhedonia: Impact of Inflammation on the Brain and Pharmacological Implications. *Pharmacol Rev* **73**, 1084-1117, doi:10.1124/pharmrev.120.000043 (2021).
93 Lalousis, P. A. *et al.* Anhedonia as a Potential Transdiagnostic Phenotype With Immune-Related Changes in Recent-Onset Mental Health Disorders. *Biol Psychiatry* **96**, 615-622, doi:10.1016/j.biopsych.2024.05.019 (2024).
94 Carpinelli, L. *et al.* Anhedonia in irritable bowel syndrome and in inflammatory bowel diseases and its relationship with abdominal pain. *Neurogastroenterol Motil* **31**, e13531, doi:10.1111/nmo.13531 (2019).
95 Krach, S., Paulus, F. M., Bodden, M. & Kircher, T. The rewarding nature of social interactions. *Front Behav Neurosci* **4**, 22, doi:10.3389/fnbeh.2010.00022 (2010).
96 Torquet, N. *et al.* Social interactions impact on the dopaminergic system and drive individuality. *Nat Commun* **9**, 3081, doi:10.1038/s41467-018-05526-5 (2018).
97 Manduca, A. *et al.* Dopaminergic Neurotransmission in the Nucleus Accumbens Modulates Social Play Behavior in Rats. *Neuropsychopharmacology* **41**, 2215-2223, doi:10.1038/npp.2016.22 (2016).
98 Han, M., Jiang, G., Luo, H. & Shao, Y. Neurobiological Bases of Social Networks. *Front Psychol* **12**, 626337, doi:10.3389/fpsyg.2021.626337 (2021).
99 Yamaguchi, Y., Lee, Y. A. & Goto, Y. Dopamine in socioecological and evolutionary perspectives: implications for psychiatric disorders. *Front Neurosci* **9**, 219, doi:10.3389/fnins.2015.00219 (2015).
100 Milaneschi, Y. *et al.* Association of inflammation with depression and anxiety: evidence for symptom-specificity and potential causality from UK Biobank and NESDA cohorts. *Mol Psychiatry* **26**, 7393-7402, doi:10.1038/s41380-021-01188-w (2021).
101 Osimo, E. F. *et al.* Inflammatory markers in depression: A meta-analysis of mean differences and variability in 5,166 patients and 5,083 controls. *Brain Behav Immun* **87**, 901-909, doi:10.1016/j.bbi.2020.02.010 (2020).
102 Isingrini, E. *et al.* Resilience to chronic stress is mediated by noradrenergic regulation of dopamine neurons. *Nat Neurosci* **19**, 560-563, doi:10.1038/nn.4245 (2016).
103 Willmore, L., Cameron, C., Yang, J., Witten, I. B. & Falkner, A. L. Behavioural and dopaminergic signatures of resilience. *Nature* **611**, 124-132, doi:10.1038/s41586-022-05328-2 (2022).
104 Falvey, A. Vagus nerve stimulation and inflammation: expanding the scope beyond cytokines. *Bioelectron Med* **8**, 19, doi:10.1186/s42234-022-00100-3 (2022).
105 Tsaava, T. *et al.* Specific vagus nerve stimulation parameters alter serum cytokine levels in the absence of inflammation. *Bioelectron Med* **6**, 8, doi:10.1186/s42234-020-00042-8 (2020).

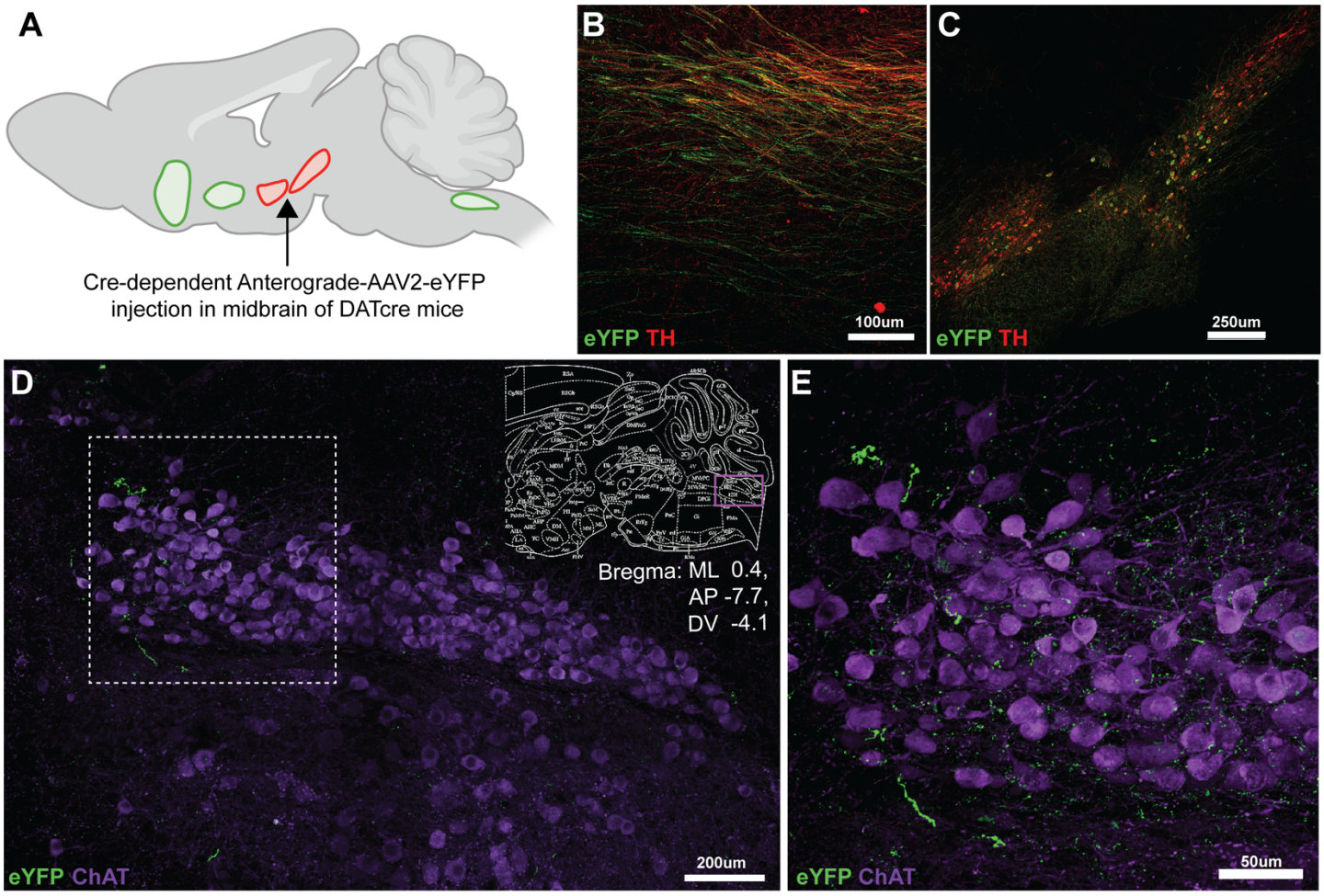

Figure 1. Anterograde tracing shows midbrain-to-dorsal vagal complex monosynaptic projections.

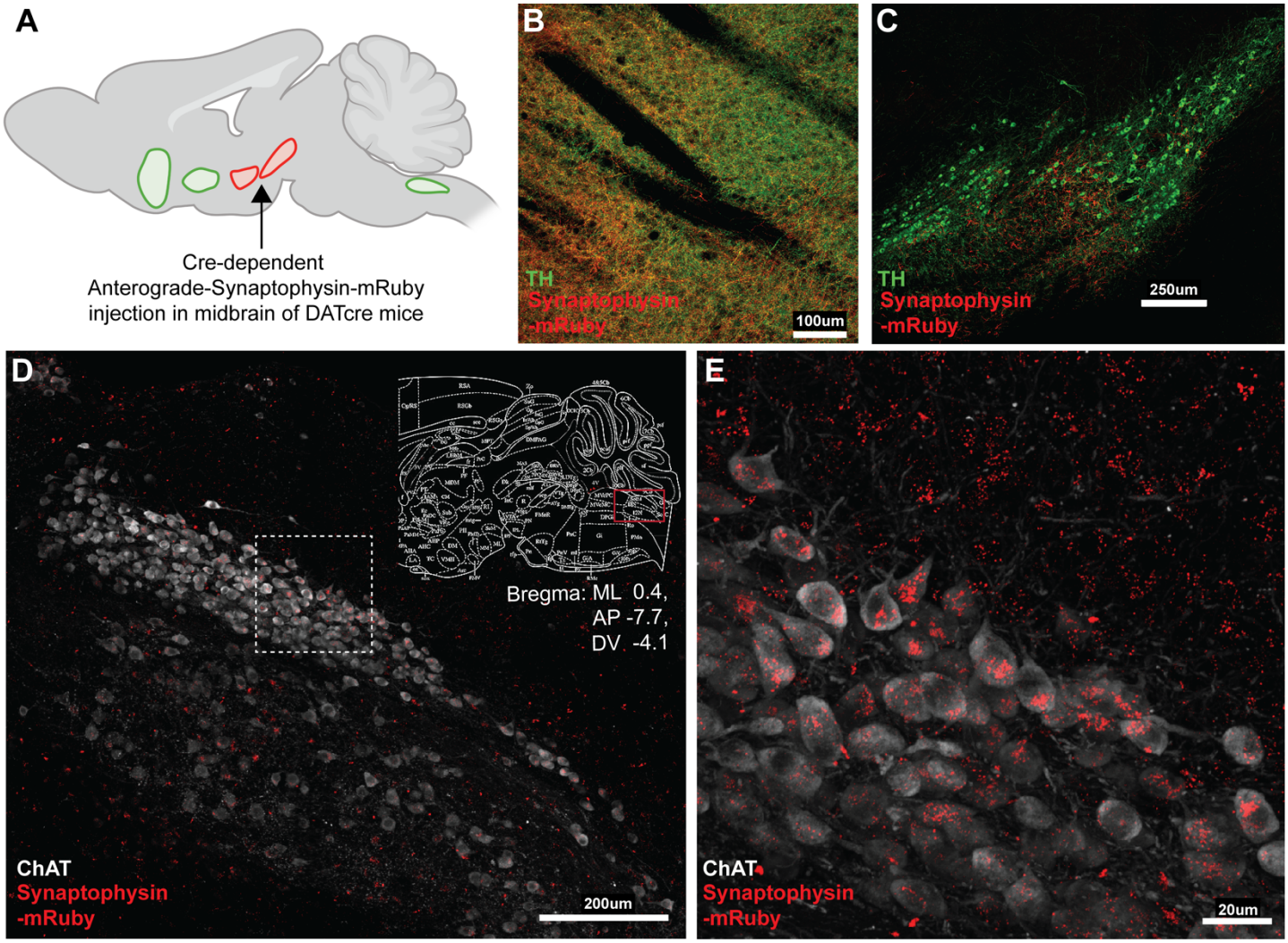

Figure 2. Neural circuit tracing data showing that DAT$^+$ midbrain neurons make synapses throughout the dorsal vagal complex.

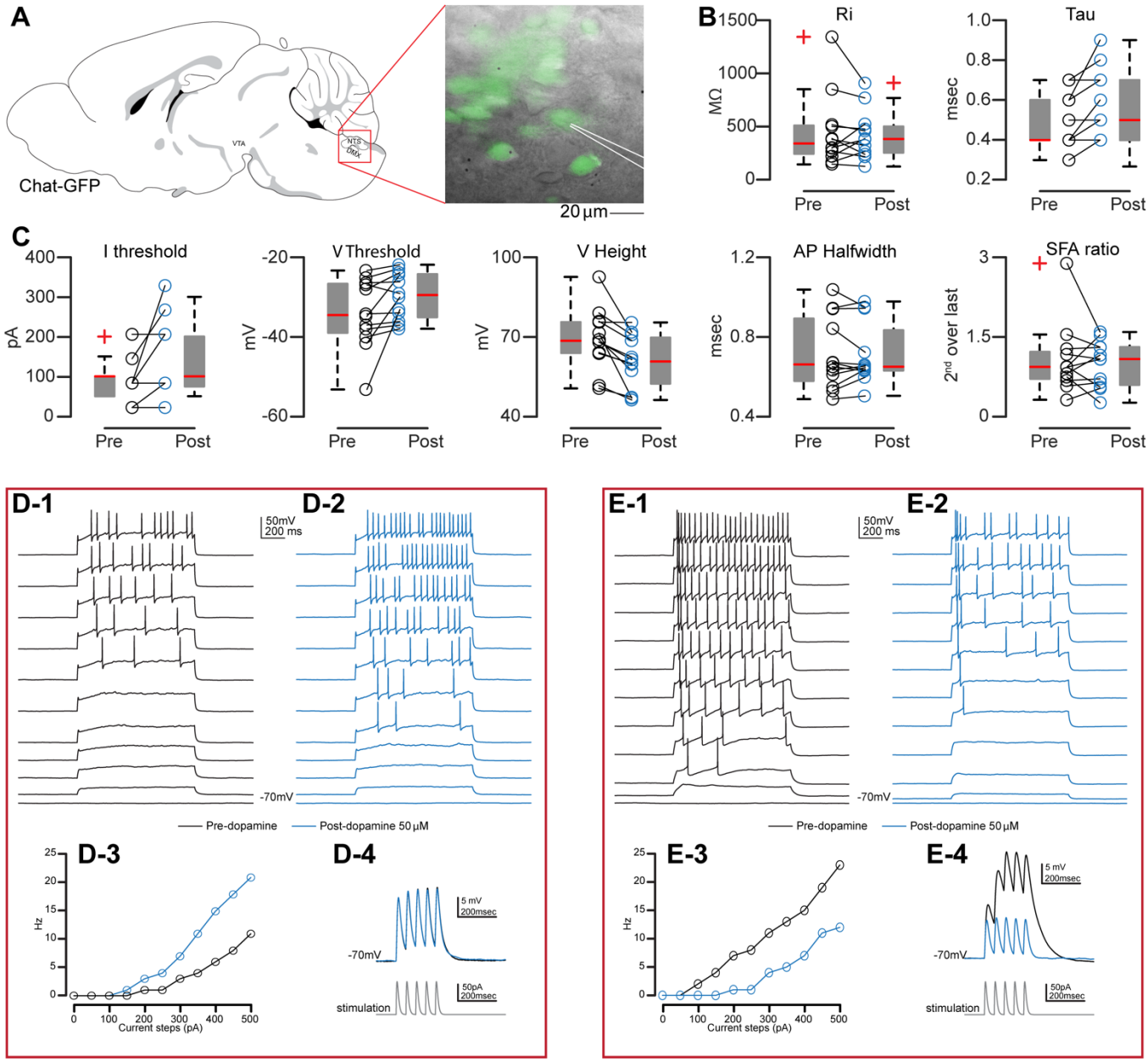

Figure 3. Electrophysiological properties of dorsal vagal complex neurons in response to Dopamine indicate presence of D1-like and D2-like receptor expression in the DVC.

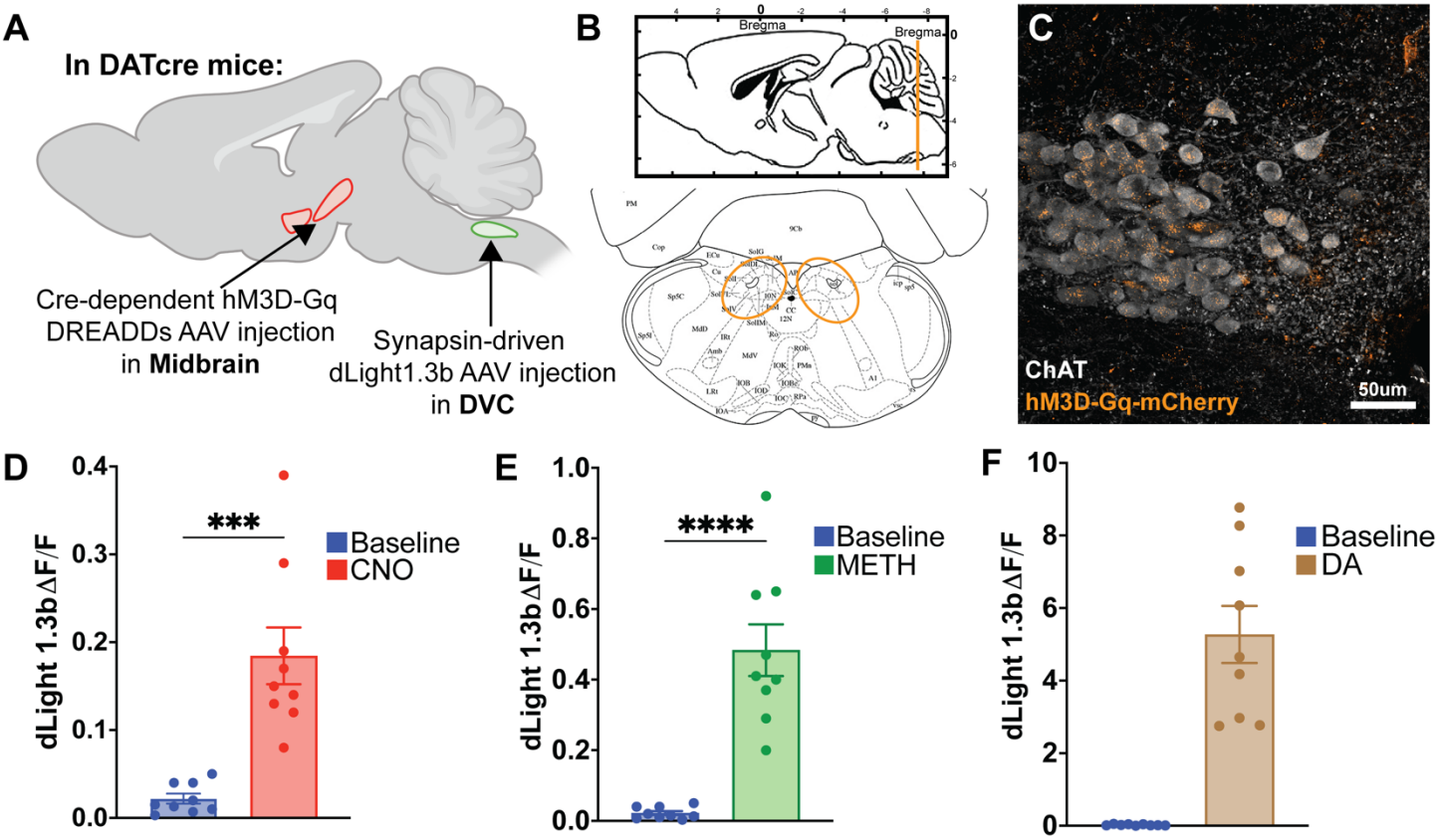

Figure 4. Midbrain dopamine neuron projections expressing excitatory DREADD receptors in the DVC release dopamine upon stimulation with CNO, and upon stimulation with methamphetamine, indicating functional projections from midbrain DAT+ neurons to DVC.

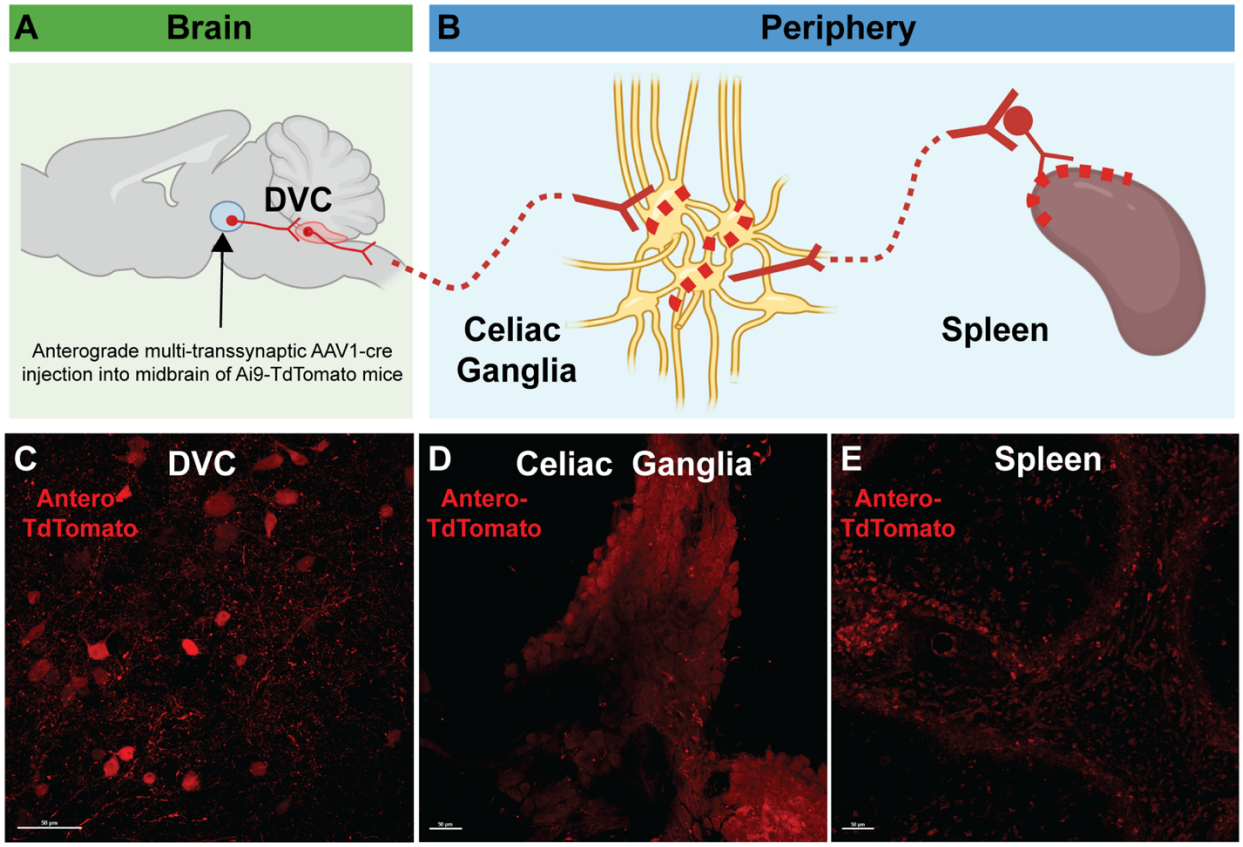

Figure 5. Anterograde multi-transsynaptic AAV tracing reveals midbrain-to-spleen connectivity via celiac ganglion.

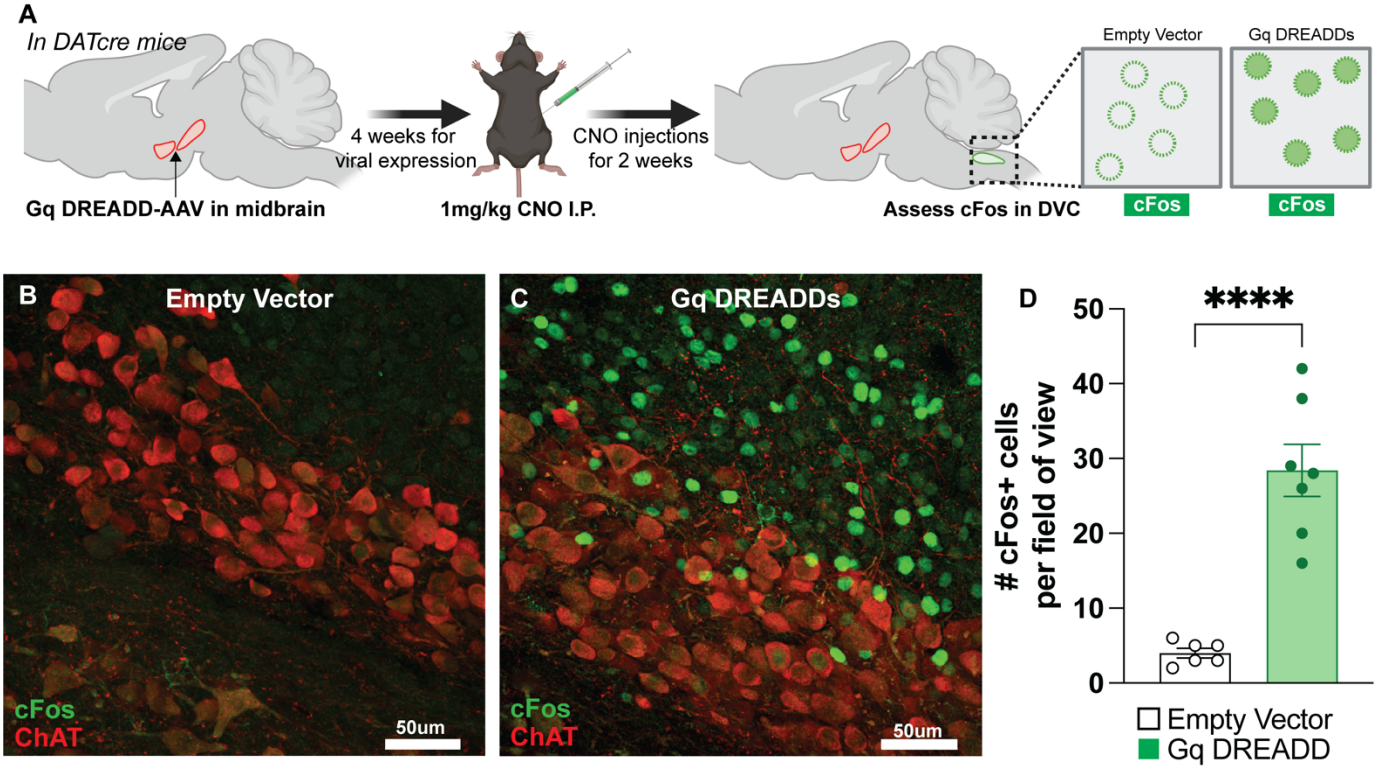

Figure 6: DREADD stimulation of midbrain dopamine neurons increases cFos expression in the DVC, indicating that dopamine neuron activation can modulate DVC activity

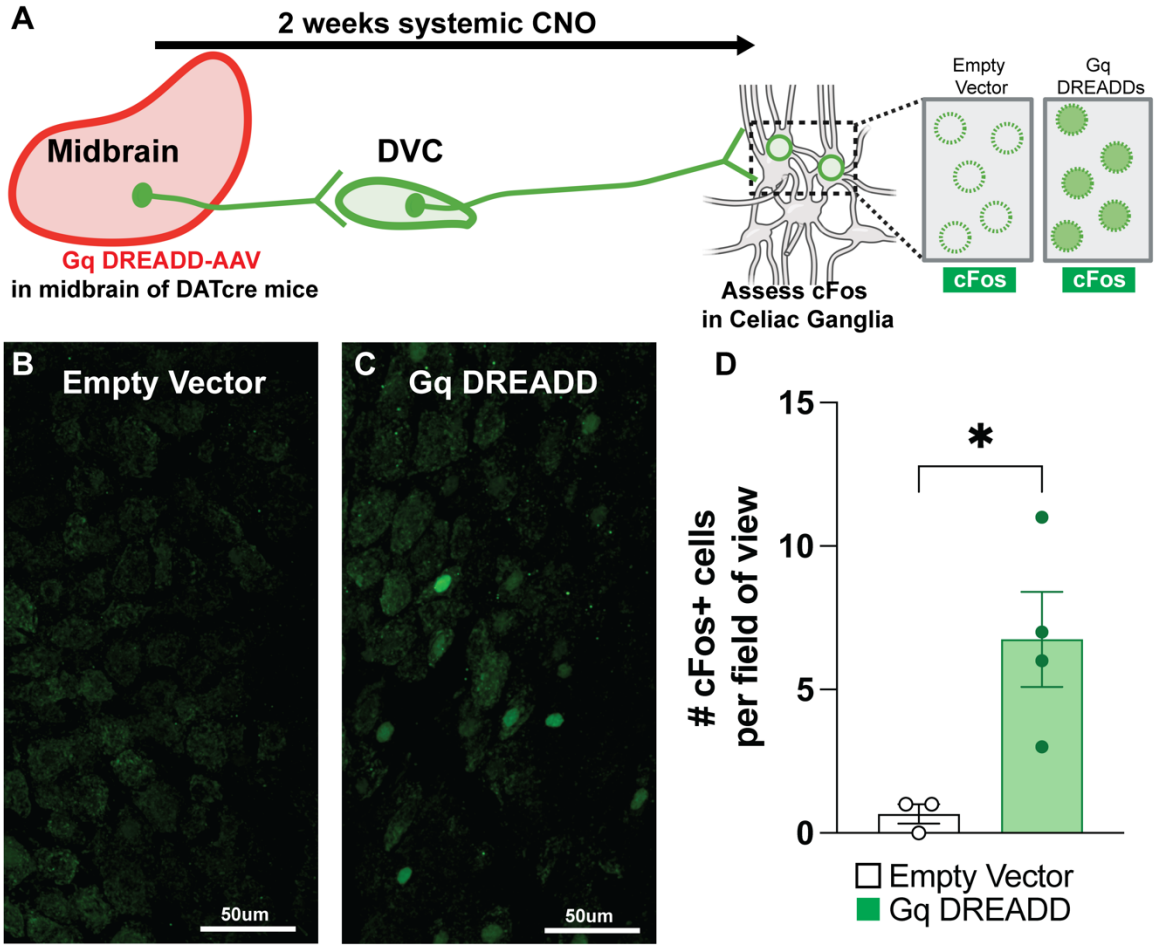

Figure 7: DREADD stimulation of midbrain dopamine neurons increases cFos expression in celiac ganglia, indicating that dopamine neuron activity can modulate celiac ganglia activity via Midbrain-DVC-celiac ganglion pathway.

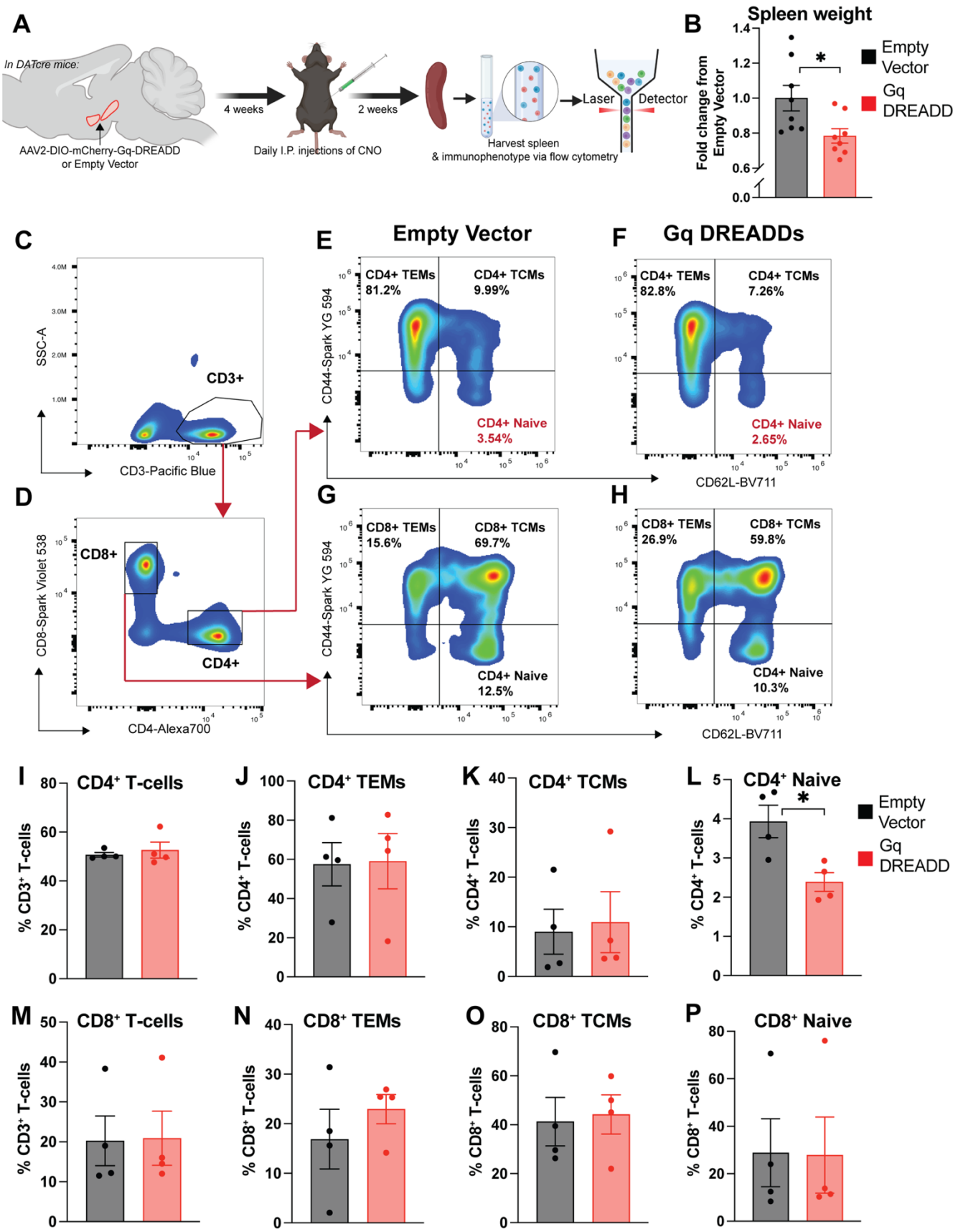

Figure 8: DREADD stimulation of midbrain dopamine neurons reduces spleen weight, and reduces naïve CD4+ T-cells in the spleen, but has no effect on CD8+ T-cell populations.

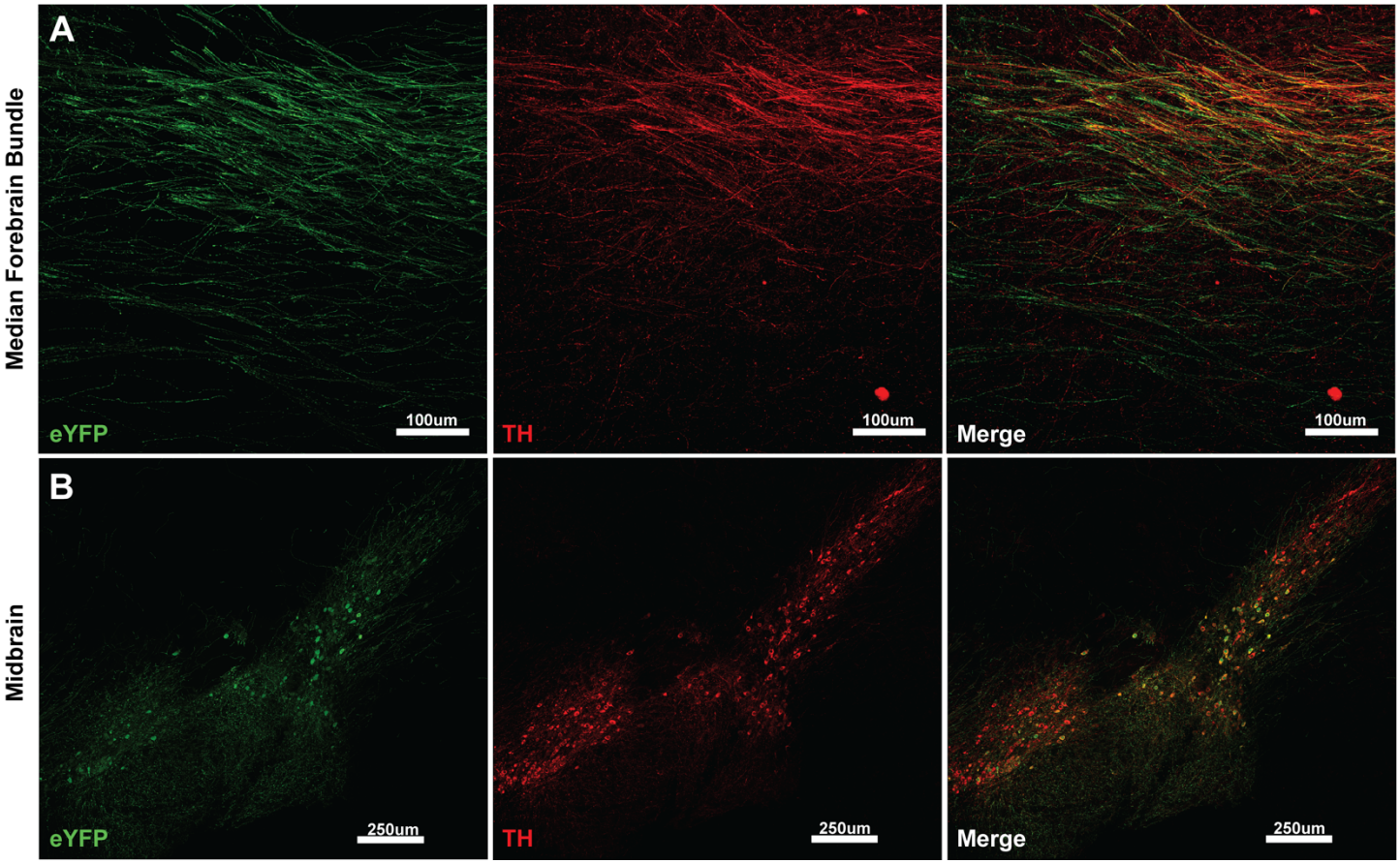

Supplementary figure 1. Single channel control images for eYFP-expressing midbrain and median forebrain bundle verify injection site and expression in midbrain dopamine neuron projections.

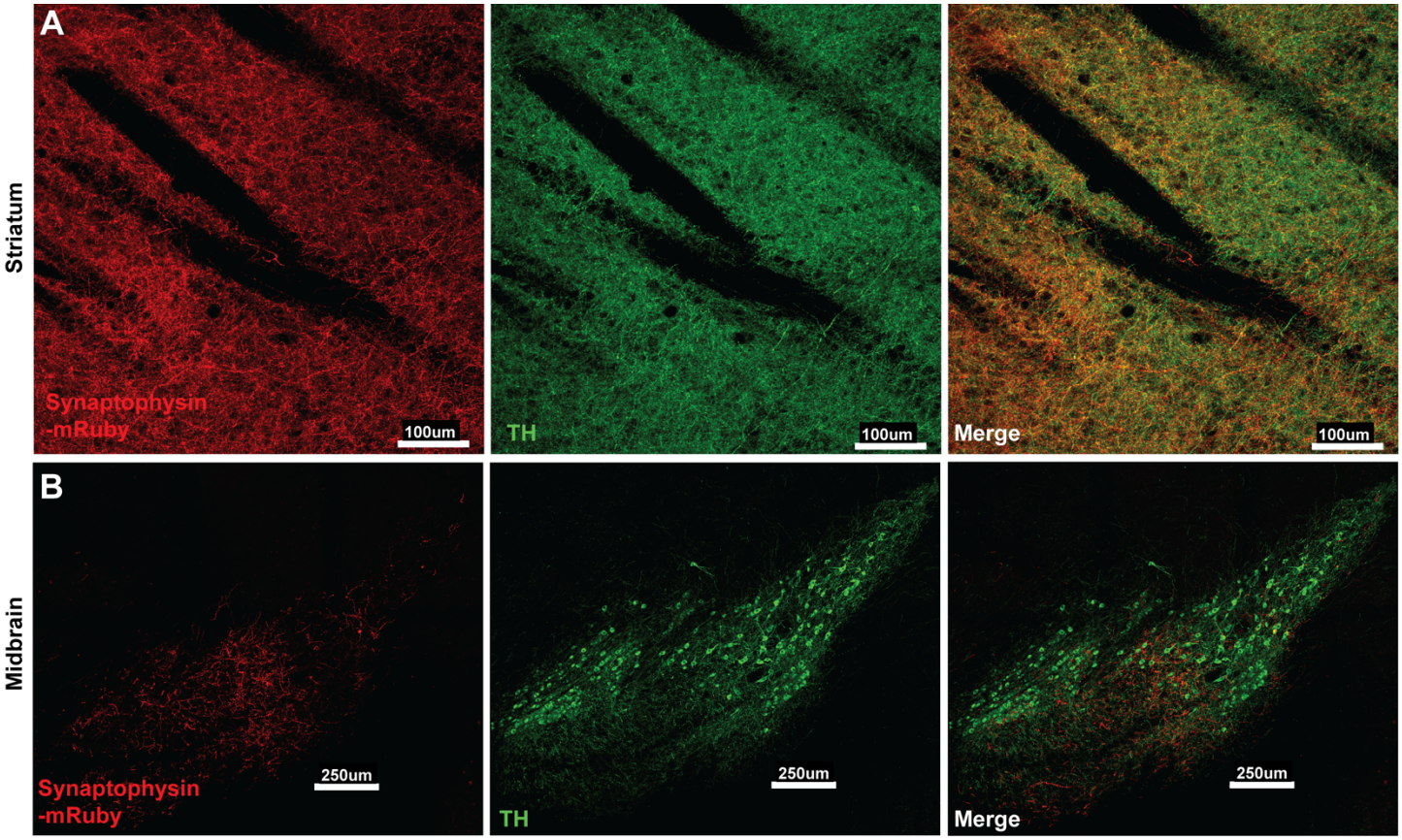

Supplementary Figure 2. Single channel control images for synaptophysin-expressing midbrain and striatum verify injection site and expression in midbrain dopamine neuron projections.

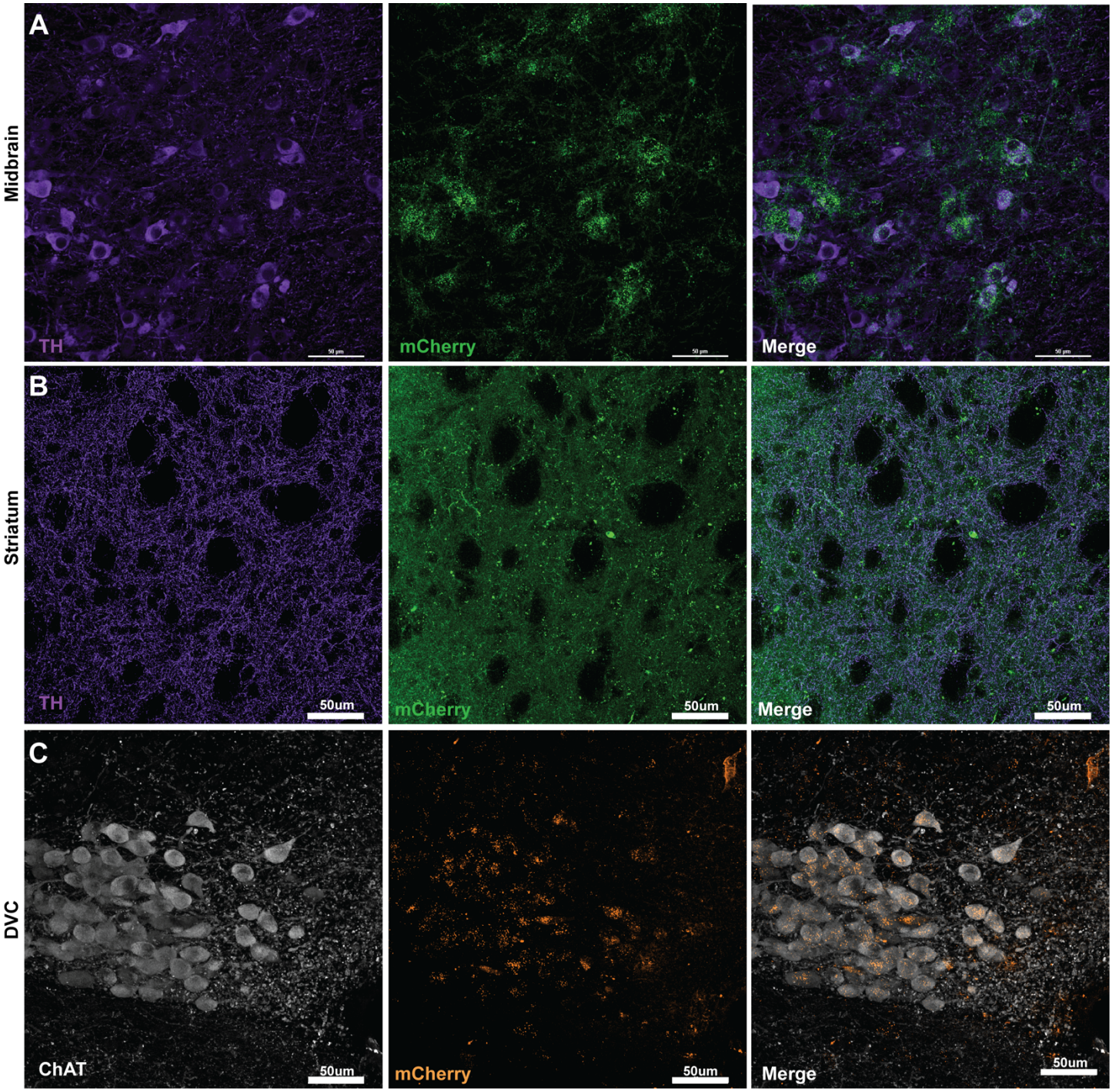

Supplementary Figure 3. mCherry-tagged Gq DREADDs under control of Cre-recombinase are expressed in midbrain dopamine neurons and terminal regions including the DVC.

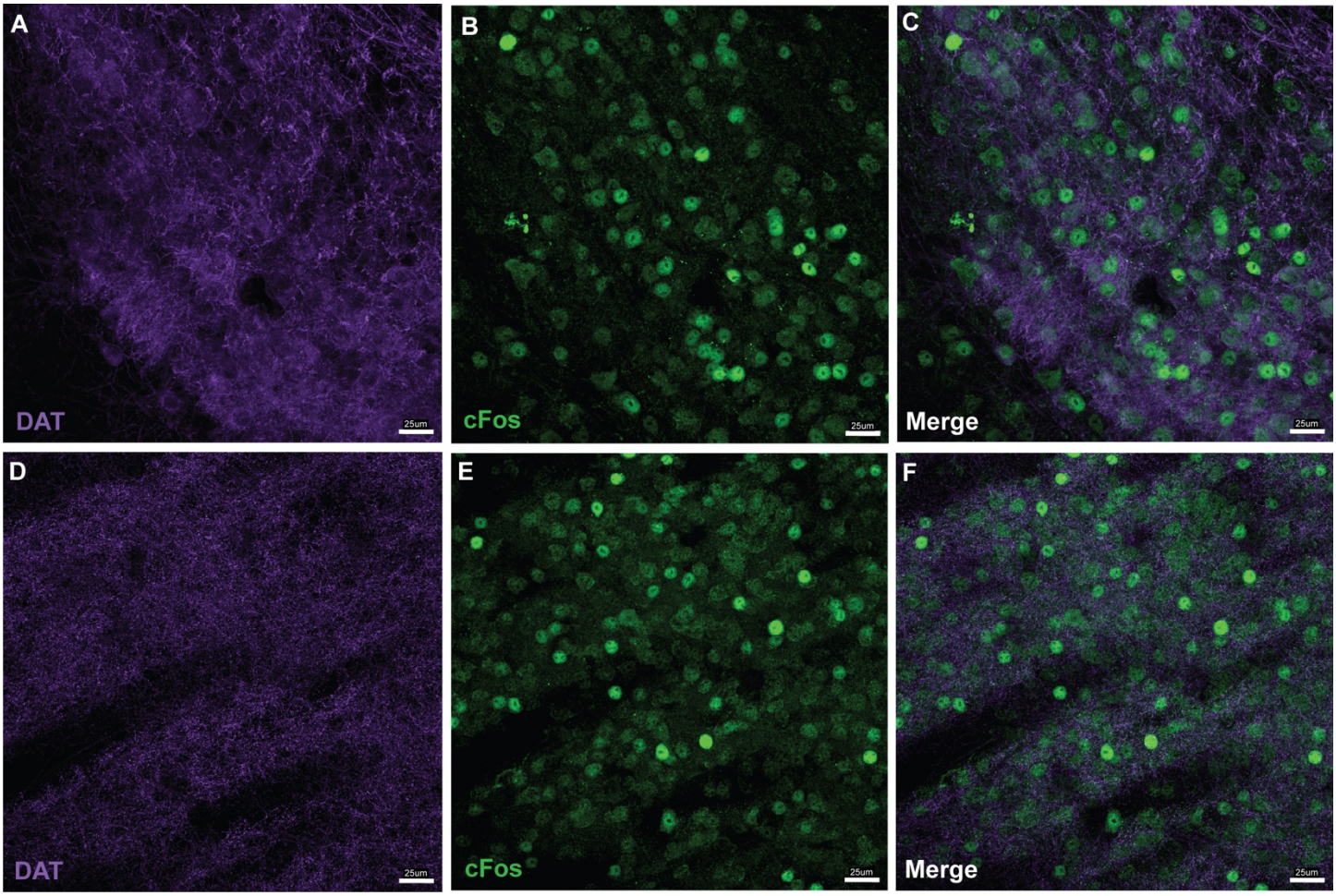

Supplementary Figure 4: Gq DREADD stimulation of midbrain dopamine neurons increases cFos expression in both midbrain and striatum

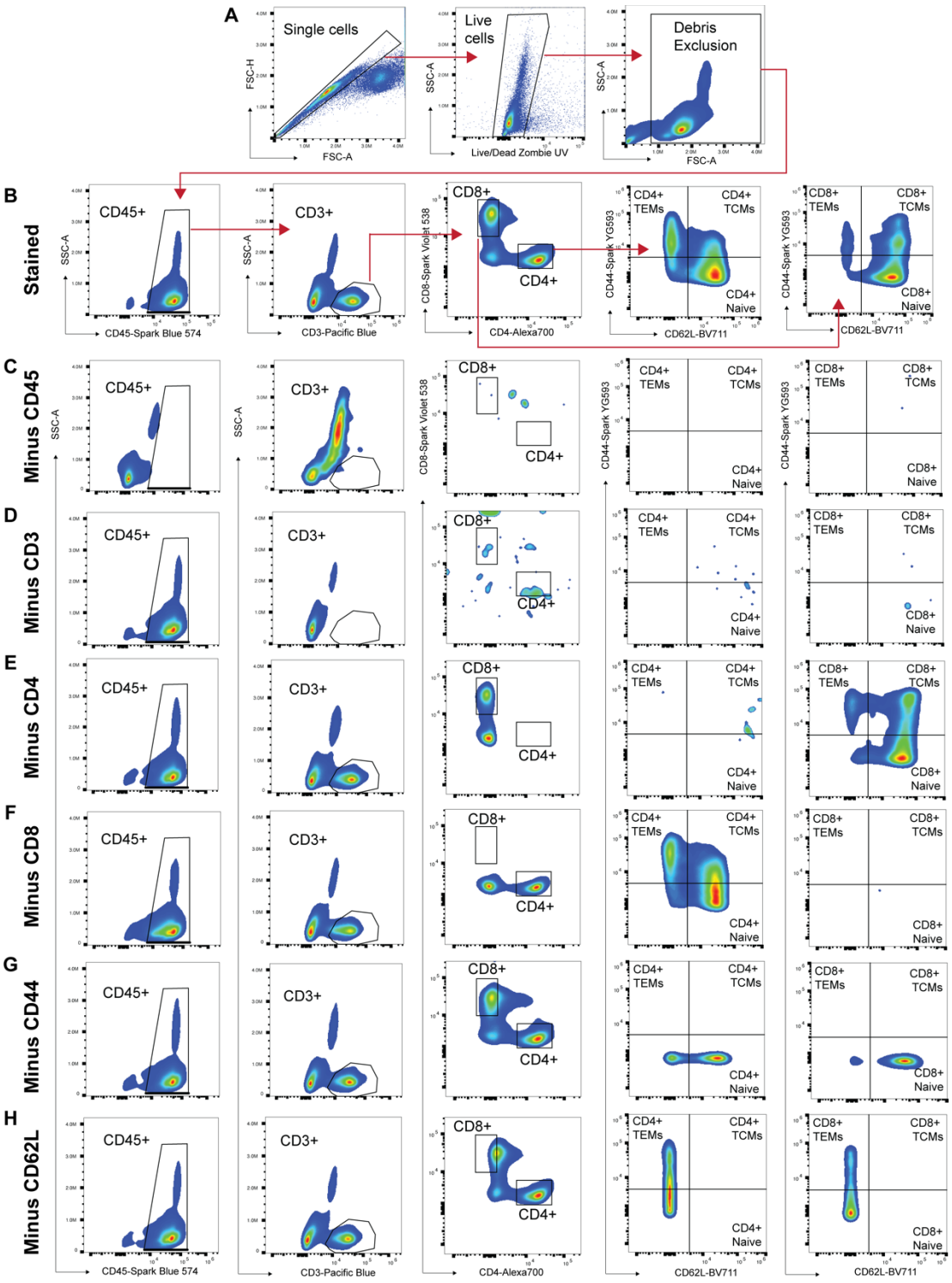

Supplementary Figure 5. Fluorescence-minus-one generated gating strategy to analyze splenic T-cell populations.

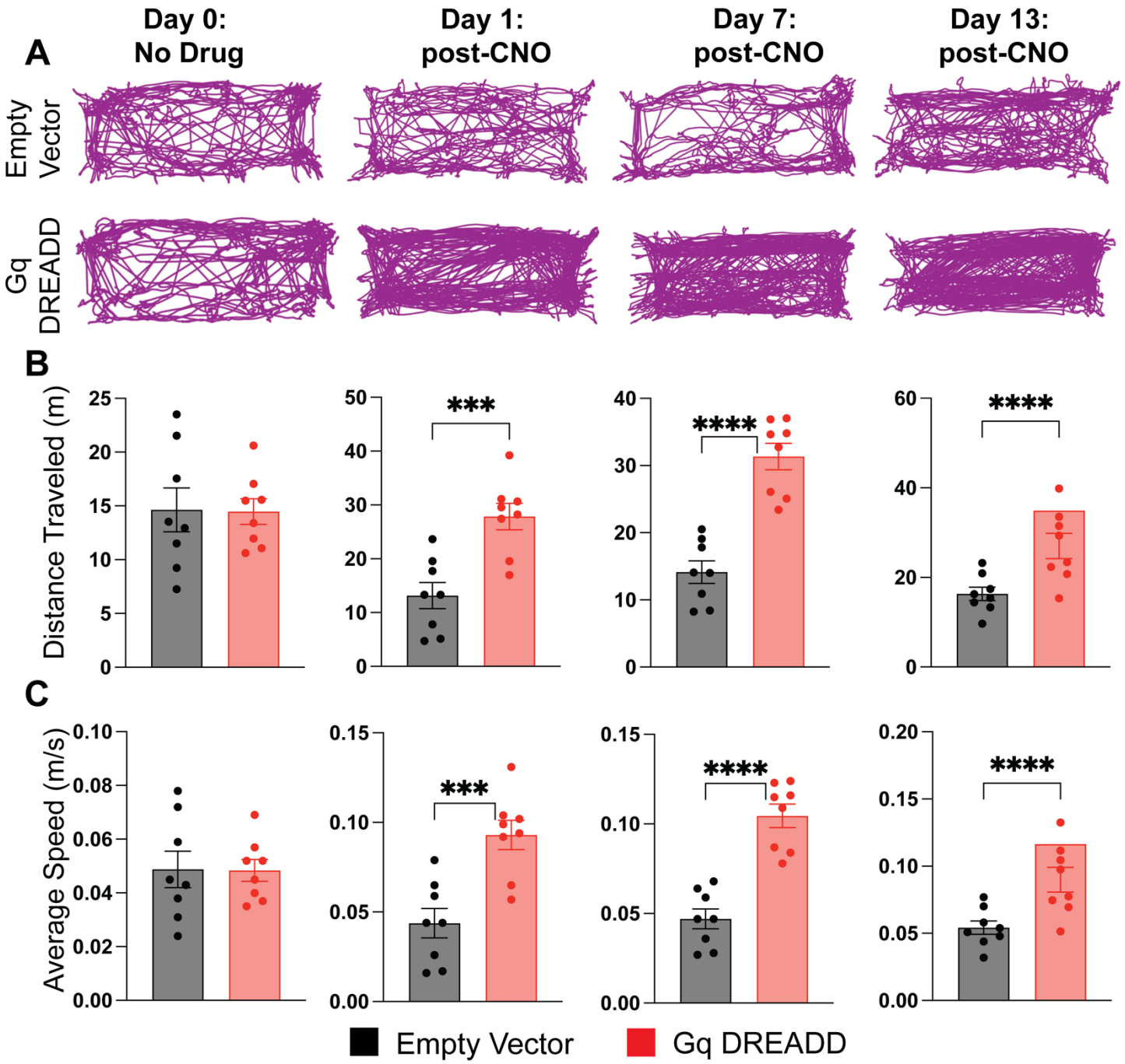

Supplemental Figure 5: Gq DREADD stimulation results in increased locomotor activity following I.P. injection of 1mg/kg CNO.

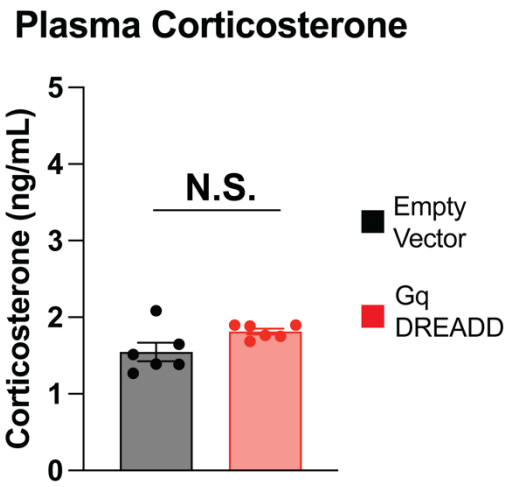

Supplementary Figure 6. Plasma corticosterone levels are not significantly changed in mice receiving midbrain Gq DREADDs compared to empty vector control.